

## The protective effect of high mobility group protein HMGA2 in pressure overload-induced cardiac remodeling



Qing-Qing Wu<sup>a,b,c</sup>, Yang Xiao<sup>a,b,c</sup>, Chen Liu<sup>a,b,c</sup>, Mingxia Duan<sup>a,b,c</sup>, Zhulan Cai<sup>a,b,c</sup>, Saiyang Xie<sup>a,b,c</sup>, Yuan Yuan<sup>a,b,c</sup>, Haiming Wu<sup>a,b,c</sup>, Wei Deng<sup>a,b,c</sup>, Qizhu Tang<sup>a,b,c,\*</sup>

<sup>a</sup> Department of Cardiology, Renmin Hospital of Wuhan University, Wuhan 430060, PR China

<sup>b</sup> Cardiovascular Research Institute, Wuhan University, Wuhan 430060, PR China

<sup>c</sup> Hubei Key Laboratory of Cardiology, Wuhan 430060, PR China

### ARTICLE INFO

#### Keywords:

HMGA2  
Cardiac remodeling  
PPAR $\gamma$   
NRF2  
C/EBP $\beta$

### ABSTRACT

High mobility group protein AT-hook 2 (HMGA2), an architectural transcription factor, has previously been reported to play an essential role in regulating the expression of many genes through architectural remodeling processes. However, the effects of HMGA2 on cardiovascular disease, especial cardiac remodeling, is unclear. This study was aimed at investigating the functional role of HMGA2 in pressure overload-induced cardiac remodeling. Mice that were subjected to aortic banding (AB) for 8 weeks developed myocardial hypertrophy and cardiac dysfunction, which were associated with altered expression of HMGA2. Cardiac-specific expression of the human HMGA2 gene in mice with an adeno-related virus 9 delivery system ameliorated cardiac remodeling and improve cardiac function in response to pressure overload by activating PPAR $\gamma$ /NRF2 signaling. Knockdown of HMGA2 by AAV9-shHMGA2 accelerated cardiac remodeling after 1 weeks of AB surgery. Additionally, knockdown of heart PPAR $\gamma$  largely abolished HMGA2 overexpression-mediated cardioprotection. HMGA2-mediated cardiomyocyte protection was largely abrogated by knocking down NRF2 and inhibiting PPAR $\gamma$  in cardiomyocytes. PPAR $\gamma$  activation was mediated by C/EBP $\beta$ , which directly interacted with HMGA2. Knocking down C/EBP $\beta$  offset the effects of HMGA2 on PPAR $\gamma$  activation and cardioprotection. These findings show that the overexpression of HMGA2 ameliorates the remodeling response to pressure overload, and they also imply that the upregulation of HMGA2 may become a treatment strategy in cardiac pathologies.

### 1. Introduction

Cardiac remodeling refers to the alterations in cardiac structure, shape, and function that result from pathophysiologic stimuli [1]. Cardiac hypertrophy, which is characterized by an increase in the thickness of the ventricular wall due to myocyte enlargement, is one of the major responses to stresses and/or myocardial injury [2]. Over time, chronic stress or disease will result in ventricular dilation and a decline in contractile function and will eventually progress to heart failure.

The high mobility group (HMG) of nuclear proteins regulates the expression of many genes through the architectural remodeling of the chromatin structure and the formation of multiprotein complexes on promoter/enhancer regions [3]. HMGA2 is a member of the HMGA subfamily of HMG proteins and functions as an architectural transcriptional factor by recognizing AT-rich sequences in the minor groove of DNA [4]. The HMGA2 protein is expressed ubiquitously and

abundantly during embryogenesis and in mesenchymal stem cells, whereas its expression is low in fully differentiated adult tissues [5]. The HMGA2 protein is upregulated in many malignant cancers, including acute myeloid leukemia [6], breast cancer [7], nonsmall cell lung cancer [8], and glioma [4]. This finding suggests that HMGA proteins regulate normal cell growth and differentiation. HMGA2 has also been reported to modulate the epithelial-mesenchymal transition in the human lens [3] as well as osteogenic differentiation [9]. Koshiro Monzen et al. have revealed the crucial role of HMGA2 in cardiogenesis [5]. Furthermore, haploinsufficiency of the HMGA1 gene, the other member of HMG family, was reported to cause cardiac hypertrophy in mice [10]. These findings indicate the potential role of HMGA2 in cardiovascular disease.

In this study, we examined whether cardiac-specific overexpression of HMGA2 influenced cardiac remodeling in the context of pressure overload. Our data indicate that HMGA2 expression is upregulated in mouse hearts at 1 week after AB surgery and then downregulated at

\* Corresponding author at: Department of Cardiology, Renmin Hospital of Wuhan University, Jiefang Road 238, Wuhan 430060, PR China.

E-mail address: [qztang@whu.edu.cn](mailto:qztang@whu.edu.cn) (Q. Tang).

<https://doi.org/10.1016/j.yjmcc.2019.01.027>

Received 8 November 2018; Received in revised form 28 January 2019; Accepted 30 January 2019

Available online 31 January 2019

0022-2828/© 2019 Elsevier Ltd. All rights reserved.

4 weeks after AB surgery. The overexpression of HMGA2 relieves the remodeling responses by activating PPAR $\gamma$  activation, which is mediated by an interaction with C/EBP $\beta$  to directly increase PPAR $\gamma$  transcription.

## 2. Materials and methods

### 2.1. Animals and animal models

All animal procedures were performed in accordance with the Guide for the Care and Use of Laboratory Animals, published by the US National Institutes of Health (NIH Publication No. 85-23, revised in 1996) and approved by the Animal Care and Use Committee of Renmin Hospital of Wuhan University (Protocol No. 00013274). Six-week-old male C57BL/6J mice were purchased from the Chinese Academy of Medical Sciences (Beijing, China). Two weeks before the AB surgery, mice were randomly chosen to receive a heart injection of either AAV9-HMGA2/AAV9-shHMGA2 (n = 15) or AAV9-negative control (AAV9-NC)/AAV9-shRNA (n = 15) at  $1 \times 10^{11}$  vp (viral particles) per animal. Then, mice were subjected to either aortic banding (AB) or a sham operation, as described previously [11]. The mice were euthanized by cervical dislocation at 8 weeks (mice receiving AAV9-HMGA2) or 1 week (mice receiving AAV9-shHMGA2) after surgery. The hearts and lungs of the euthanized mice were harvested and weighed to compare the heart weight/body weight (HW/BW, mg/g), lung weight/body weight (LW/BW, mg/g), and heart weight/tibia length (HW/TL, mg/mm) ratios.

To knockdown PPAR $\gamma$ , mice were subjected to a myocardial injection of AAV9-shPPAR $\gamma$  ( $1 \times 10^{11}$  vp per mouse) two weeks before the AB procedure.

### 2.2. Recombinant adeno-associated virus (AAV)9-HMGA2 Construct

AAV9-HMGA2 and AAV9-NC were constructed and generated by Vigene Biosciences (Shandong, China). The HMGA2 expression cassette consists of a CMV promoter followed by the human HMGA2 coding sequence. The HMGA2 gene was cloned into a p-ENTER vector by the AsiS I and Mlu I restriction sites. The p-ENTER plasmid containing the desired gene and AAV vectors pAV-C-GFP were cotransfected into 293 cells to obtain the pAAV-MCS plasmid by homologous recombination to recombine the target gene into the pAV-C-GFP vector. Then, the recombinant plasmid pAAV-MCS together with Helper (carrying the adenovirus-derived gene) and pAAV-RC (carrying the AAV replication and capsid genes) were cotransfected into the AAV-293 cells (To provide a trans-acting factor for AAV replication and

packaging). Three days after transfection, AAV9 vector-producing 293T cells were harvested for vector purification. Viral stocks were obtained by CsCl<sub>2</sub>-gradient centrifugation. Titration of AAV viral particles was performed by real-time PCR quantification of the number of viral genomes, as measured by the CMV copy number. The viral preparations had titers between  $1 \times 10^{13}$  and  $5 \times 10^{13}$  vg per mL.

The AAV9-shPPAR $\gamma$  and the scramble RNA (AAV9-shRNA) were constructed by Vigene Bioscience (Shanghai, China) with PPAR $\gamma$  siRNA purchased from Santa Cruz (sc-29456).

The AAV9-shHMGA2 and the scramble RNA (AAV9-shRNA) were constructed by Vigene Bioscience (Shanghai, China) with HMGA2 siRNA purchased from Thermo Fisher (AM16708).

### 2.3. Viral delivery protocol

Two weeks before the AB surgery, mice were randomly chosen to receive a heart injection of either AAV9-HMGA2 /AAV9-shHMGA2/ AAV9-shPPAR $\gamma$  (n = 15) or AAV9-NC/AAV9-shRNA (n = 15) at  $1 \times 10^{11}$  vp (viral particles) per animal. Briefly, after they were anesthetized with 3% sodium pentobarbital (80 mg/kg, intraperitoneal injection), mice were placed in a supine position with a heating pad and orally intubated. Artificial respiration was maintained with a rodent ventilator. The heart was exposed upon opening the left pleural cavity by cutting the left third and fourth ribs and intercostal muscles with a cautery pen. The pericardium was removed, and a 250- $\mu$ L 29-gauge syringe was loaded with a 50  $\mu$ L injection volume. The injection sites were located on the left ventricular apex, anterior wall, and lateral wall. A single injection was performed in the apex, and two injections were performed for each of the anterior and lateral walls. Injections were spaced approximately 5 mm apart. After slowly injecting a total of 50  $\mu$ L of AAV vector ( $1 \times 10^{11}$  vp) or saline, the chest was closed in layers, and a total of 0.1 mL 0.5% bupivacaine was injected subcutaneously near both edges of the skin incision to alleviate postoperative pain. Echocardiographic measurements and invasive hemodynamic measurements were performed at 8 weeks (mice receiving AAV9-HMGA2), 1 week (mice receiving AAV9-shHMGA2) or 4 weeks (mice receiving AAV9-shPPAR $\gamma$ ) after the AB surgery, and the animals were killed.

### 2.4. Echocardiography and hemodynamics

Echocardiography was performed on anesthetized (1.5% isoflurane) mice using a MyLab 30CV ultrasound (Biosound Esaote) with a 10-MHz linear array ultrasound transducer. The left ventricle (LV) was assessed in both parasternal long-axis and short-axis views at a frame rate of 120 Hz. End-systole and end-diastole were defined as the phases in

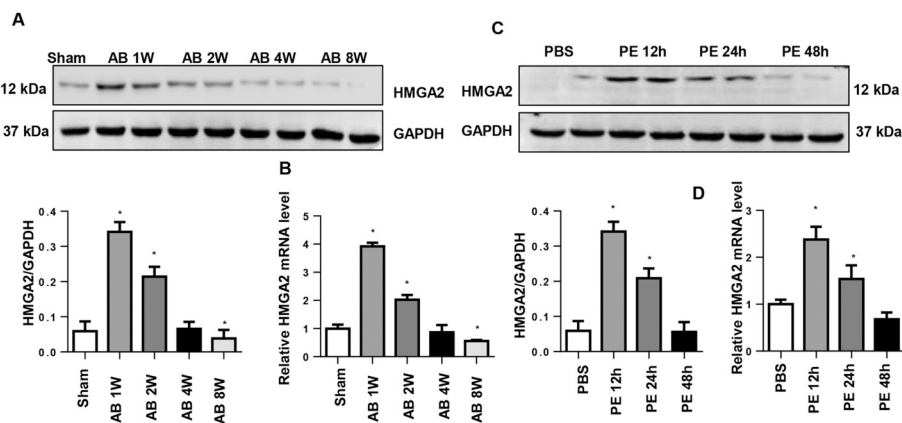
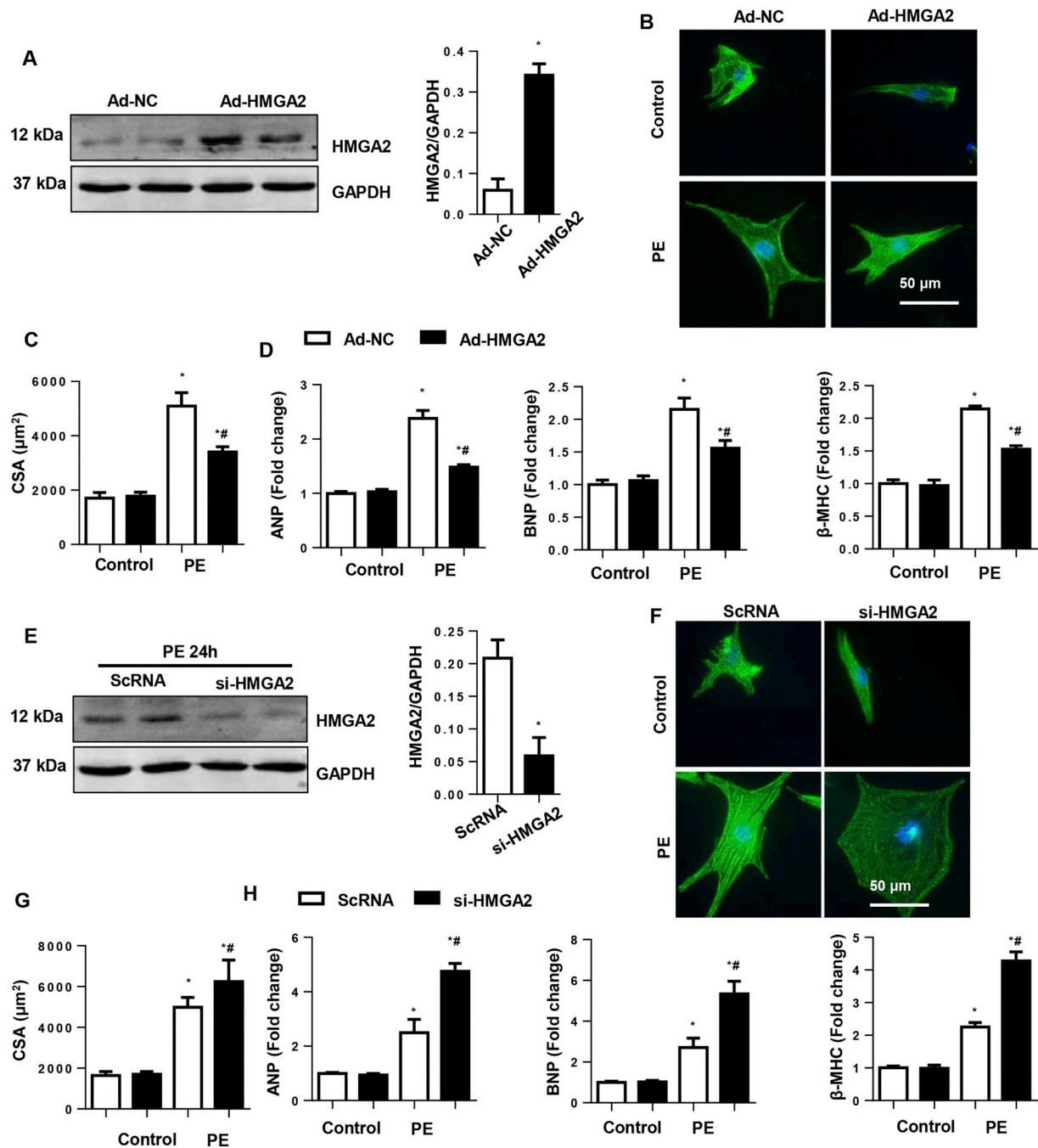


Fig. 1. The expression level of HMGA2 in cardiac remodeling.

A. HMGA2 protein expression level in mouse hearts after AB surgery (n = 6). B. HMGA2 mRNA expression levels in mouse hearts after AB surgery (n = 6, \*P < 0.05 vs. sham group). C. HMGA2 protein expression levels in cardiomyocytes after PE stimulation (n = 6). D. HMGA2 mRNA expression levels in cardiomyocytes after PE stimulation (n = 6, \*P < 0.05 vs. PBS group).

which the smallest and largest areas of the LV were obtained. The LV end-systolic diameter and LV end-diastolic diameter were measured via LV M-mode tracing with a sweep speed of 50 mm/s at the midpapillary muscle level.

Hemodynamics were measured in anesthetized (1.5% isoflurane) mice using cardiac catheterization. A microtip catheter transducer (SPR-839; Millar Instruments, Houston, TX) was inserted into the right carotid artery and advanced into the LV. Fifteen minutes after



**Fig. 2.** HMGGA2 overexpression relieves PE induced cardiac remodeling *in vitro*.

A-D. NRCMs were transfected with Ad-HMGA2 and then stimulated with PE for 48 h. A. HMGGA2 protein expression level after the cells were transfected with Ad-HMGA2 (n = 6, \*P < 0.05 vs. Ad-NC group). B and C.  $\alpha$ -actin staining (B) and quantitative results (C) for the detection of cell surface area in the indicated groups (n > 50 cells per group). D. Transcription of hypertrophic markers in the indicated groups (n = 6). \*P < 0.05 vs. the corresponding control group; # P < 0.05 vs. the Ad-NC-PE group.

E-H. NRCMs were stimulated with PE for 24 h and then transfected with HMGGA2 siRNA. E. HMGGA2 protein expression levels after the cells were transfected with HMGGA2 siRNA (n = 6, \*P < 0.05 vs. the ScRNA group). F and G.  $\alpha$ -actin staining (F) and quantitative results (G) for the detection of cell surface area in the indicated groups (n > 50 cells per group). H. Transcription of hypertrophic markers in the indicated groups (n = 6). \*P < 0.05 vs. the corresponding control group; # P < 0.05 vs. the ScRNA-PE group.

stabilization, pressure signals and heart rate were continuously recorded with a Millar Pressure-Volume System (MPVS-400; Millar Instruments) coupled with a Powerlab/4SP A/D converter and then stored and displayed on a personal computer. Data were processed using the PVAN data analysis software.

## 2.5. Histological analysis

Hematoxylin–eosin and Picrosirius Red staining, immunohistochemical analysis and TUNEL staining were performed as previously described [12,13]. The 4-hydroxynonenol antibody was used for immunohistochemical staining.

## 2.6. Cell culture and treatment

Neonatal rat cardiomyocytes (NRCMs) were isolated and cultured according to our previous study [12]. Cells were transfected with adenovirus (Ad-) to overexpress HMGA2 (Ad-HMGA2, MOI = 50,

Vigene Bioscience, Jinan China) for 8 h. Then, the cells were stimulated with 50  $\mu$ M phenylephrine (PE). To knock down the target genes, HMGA2 siRNA (AM16708, Thermo Fisher), NRF2 siRNA (Santa Cruz, sc-156,128), and C/EBP $\beta$  siRNA (AM16708, Thermo Fisher) were used. All of the cells were transfected using Lipofectamine 3000 (Thermo Fisher Scientific) according to the manufacturer's instructions. To inhibit PPAR $\gamma$ , cells were treated with GW9662 (10  $\mu$ M, Medchem Express) for 12 h. To activate PPAR $\gamma$ , cells were treated with rosiglitazone (BRL49653, 1  $\mu$ M) for 2 h. Experiments were performed three times in duplicate.

## 2.7. Real-time PCR and western blot

Real-time PCR and western blotting were performed as described in a previous study [14]. The primary antibodies that were used were HMGA2, P67, gp91, SOD, PPAR $\alpha$ , PPAR $\gamma$ , PPAR $\delta$ , PGC-1 $\alpha$ , NRF2 and laminin B, and they were purchased from Abcam (1:1000 dilution); GAPDH was purchased from Santa Cruz (1:200 dilution).

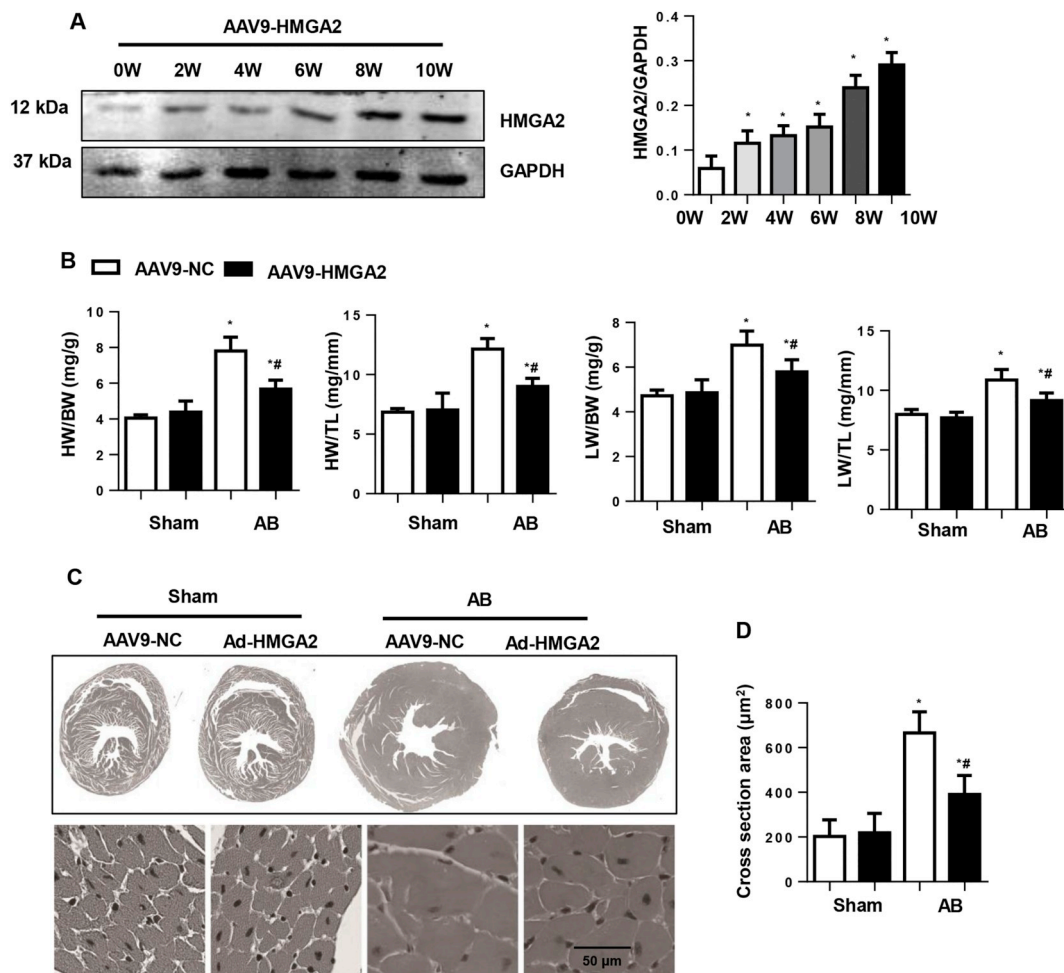


**Fig. 3.** HMGA2 overexpression suppresses pressure overload-induced cardiac remodeling in mice.

A. HMGA2 protein expression levels in mouse hearts at 0, 2, 4, 6, 8, 10 weeks after they were injected with AAV9-HMGA2 ( $n = 6$ , \* $P < 0.05$  vs. the AAV9-NC group). B. HW/BW, HW/TL, LW/BW, and LW/TL in mouse hearts 8 weeks after the AB surgery ( $n = 10$ ). C. HE staining in the indicated groups ( $n = 6$ ). D. Quantitative measurements of the cross-sectional area of cardiomyocytes in the indicated groups ( $n = 100$ – $200$  left ventricular cells). E. Transcription of hypertrophic markers in the indicated mouse hearts ( $n = 6$ ). F. PSR staining to detect collagen accumulation ( $n = 6$ ). G. Quantitative results of the left ventricular collagen volume in the indicated groups ( $n = 6$ ). H. Transcription of fibrosis markers in the indicated mouse hearts ( $n = 6$ ). \* $P < 0.05$  vs. the corresponding sham group; # $P < 0.05$  vs. the AAV9-NC-AB group.

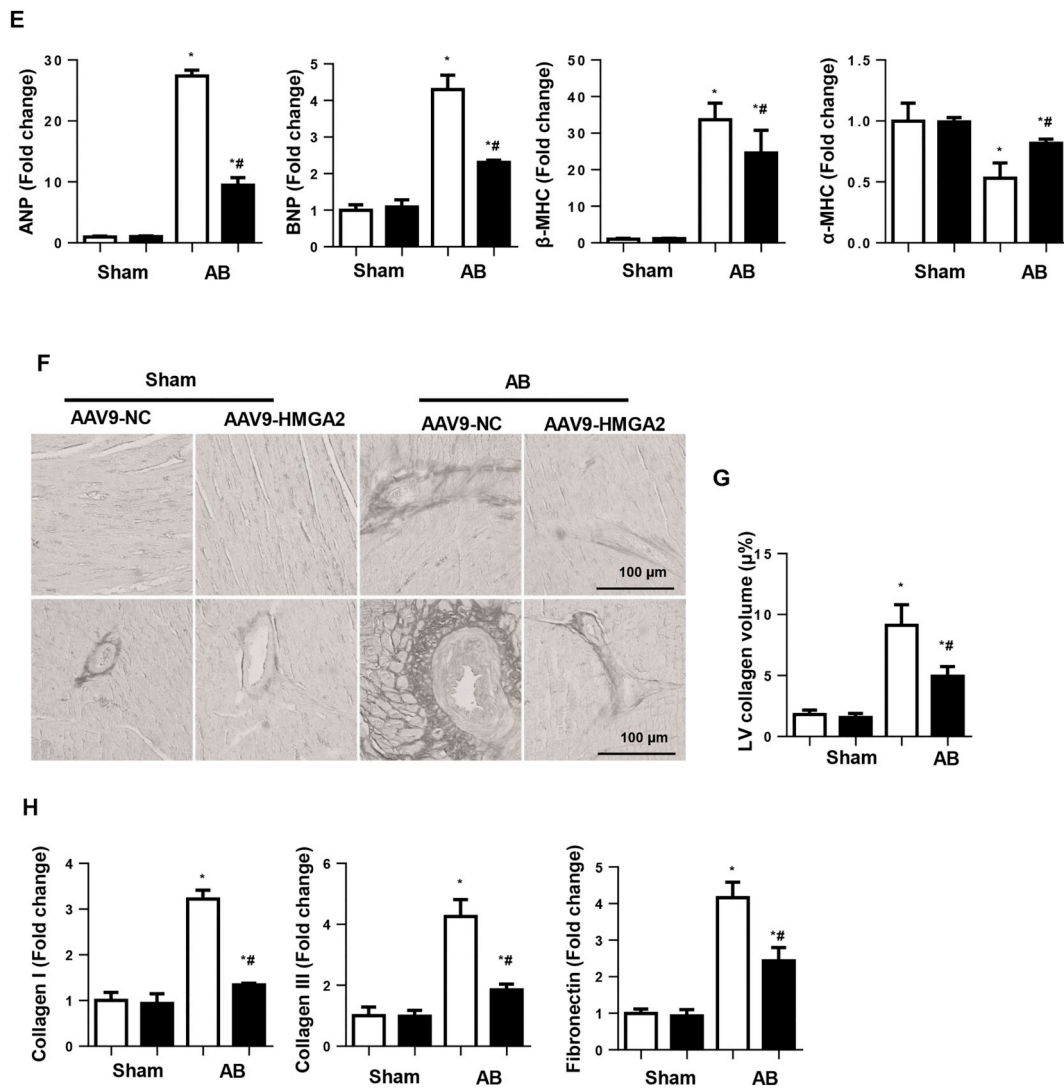


Fig. 3. (continued)

### 2.8. Detection of oxidative stress

Commercial kits (Beyotime Biotechnology, China) were used to detect the activity of SOD and NADPH oxidase and the malondialdehyde (MDA) content in fresh mouse hearts (80–120 mg) after the cardiomyocytes were lysed. A DCFH-DA probe was used to detect the ROS level with a fluorescence microplate reader.

### 2.9. Coimmunoprecipitation assays

Cultured NRCMs cotransfected with psicoR-HA-HMGA2 and psicoR-Flag-PPAR $\gamma$  or psicoR-Flag-C/EBP $\beta$ , and they were lysed in an immunoprecipitation buffer. For the immunoprecipitation procedure, 10  $\mu$ L of protein A/G-agarose beads and 1  $\mu$ g of antibody were incubated with each sample (50  $\mu$ L) overnight at 4  $^{\circ}$ C. After washing with immunoprecipitation buffer, the eluted proteins were immunoblotted with the indicated primary antibodies.

### 2.10. Luciferase assay

The luciferase reporter plasmid PPRE-LUC [containing three copies of PPRE (PPAR response elements) consensus sequence] was used.

HEK293T cells were transfected with a peroxisome proliferator response elements (PPRE)-luc plasmid in combination with Ad-HMGA2 or Ad-C/EBP $\beta$  or HMGA2 siRNA. The luciferase activity was determined with the Dual Luciferase Reporter Assay Kit (Promega) according to the manufacturer's instruction.

### 2.11. Statistical analysis

The data were analyzed with SPSS 23.3. The data are presented as the means  $\pm$  SD. Comparisons between groups were analyzed by two-way ANOVA followed by a *post hoc* Tukey test. Comparisons between two groups were analyzed by Student's unpaired *t*-test. A *p*-value less than 0.05 (two-tailed) was considered statistically significant.

## 3. Results

### 3.1. The expression level of HMGA2 in cardiac remodeling

We first detected the expression level of HMGA2 in normal hearts and diseased hearts in mice. As a result, the expression level of HMGA2 was very low in normal hearts, but it was increased in the mouse hearts at 1 week to 2 weeks after the AB surgery then quickly declined at

4 weeks to 8 weeks after the AB surgery (Fig. 1A and B). To confirm the expression level of HMGA2 in cardiomyocytes, the NRCMs were isolated and stimulated with PE for 12, 24, and 48 h. Consistent with the *in vivo* results, the expression level of HMGA2 was very low in cardiomyocytes in the physiological condition, but it increased from 12 h until 24 h after PE stimulation then dropped at 48 h after PE stimulation (Fig. 1C and D). These results indicate that HMGA2 may participate in the cardiac remodeling process during pathological insult.

### 3.2. HMGA2 overexpression relieves PE-induced cardiac remodeling *in vitro*

To investigate the functional role of HMGA2 in cardiac remodeling, the NRCMs were transfected with adenovirus (Ad) to overexpress HMGA2 (Fig. 2A). After PE stimulation for 48 h, the NRCMs revealed a significant hypertrophic response, as evidenced by their increased cell surface area (CSA) and augmented transcription level of hypertrophic markers [atrial natriuretic peptide (ANP), brain natriuretic peptide (BNP), and myosin heavy chain beta ( $\beta$ -MHC)] (Fig. 2B–D). In contrast, HMGA2 overexpression attenuated this PE-induced hypertrophic response (Fig. 2B–D). Notably, HMGA2 overexpression did not affect the cardiomyocyte function under physiological conditions, while the

HMGA2 expression level was increased at 12–24 h after PE stimulation. We stimulated the NRCMs with PE for 24 h then knocked down HMGA2 with siRNA (Fig. 2E). As a result, HMGA2 silencing caused a deteriorated cardiac hypertrophic response to PE (Fig. 2F–H). However, HMGA2 silencing did not affect the cardiomyocyte function under physiological conditions. This finding suggested that HMGA2 may protect against cardiomyocyte remodeling processes.

### 3.3. HMGA2 overexpression suppresses pressure overload-induced cardiac remodeling *in mice*

To confirm the functional role of HMGA2 in cardiac remodeling *in vivo*, the mice were subjected to a myocardial injection of AAV9-HMGA2 to overexpress HMGA2 two weeks before AB (Fig. 3A). Eight weeks after the AB surgery, the hypertrophic response was suppressed in the AAV9-HMGA2 group when compared with that of the AAV9-NC group as evidenced by their decreased heart weight (HW) to body weight (BW) ratio, HW to tibia length (TL) ratio, lung weight (LW) to BW ratio, reduced cross section area, and decreased transcription levels of hypertrophic markers (Fig. 3B–E). The overexpression of HMGA2 also attenuated pressure overload-induced fibrosis as evidenced by the

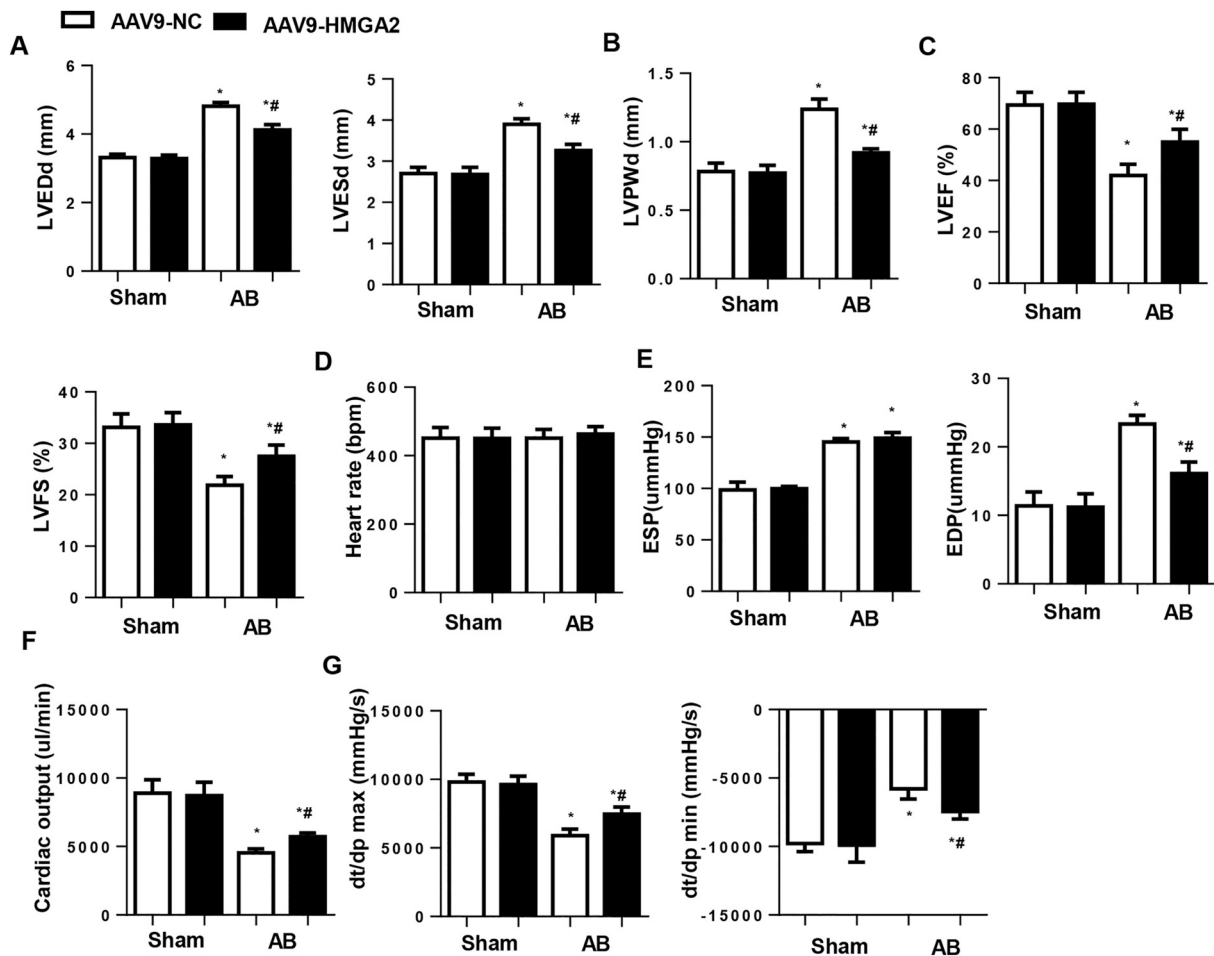


Fig. 4. HMGA2 overexpression improves cardiac function in mice undergoing cardiac remodeling.

A–G. Echocardiography and pressure volume loop were evaluated in mouse hearts after 8 weeks of AB ( $n = 8$ ). A. Left ventricular end diastolic diameter (LVEDd) and left ventricular end systolic diameter (LVESd). B. Left ventricular posterior wall diameter (LVPWd). C. Left ventricular ejection fraction (LVEF) and LV shortening fraction (LVFS). D. Heart rate. E. End systolic pressure (ESP) and end diastolic pressure (EDP). F. Cardiac output. G. Left ventricular pressure maximal rate of rise and fall ( $dp/dt_{max}$  and  $dp/dt_{min}$ ). \* $P < 0.05$  vs. the corresponding sham group; #  $P < 0.05$  vs. the AAV9-NC-AB group.

decreased left ventricular (LV) collagen volume and reduced transcription levels of fibrosis markers (collagen I, collagen III, and fibronectin) (Fig. 3E–H). Interestingly, HMGA2 overexpression in the heart did not affect cardiac geometry under physiological conditions.

### 3.4. HMGA2 overexpression improves cardiac remodeling functions in mice

Cardiac function was evaluated by echocardiography and pressure-volume loop measurement 8 weeks after the AB surgery. Pressure

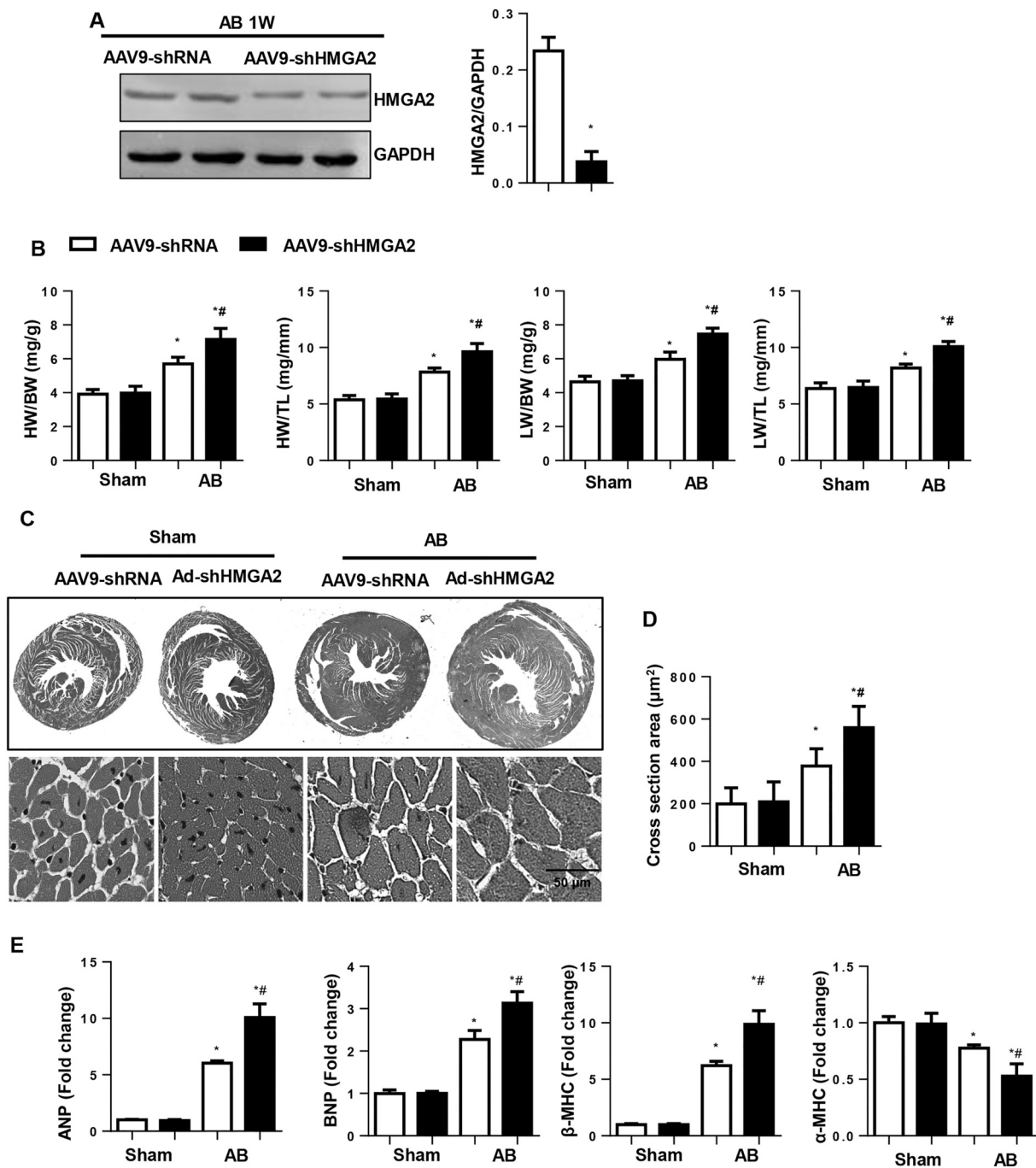


**Fig. 5.** HMGA2 knockdown accelerates cardiac hypertrophy and dysfunction.

A. HMGA2 protein expression levels in mouse hearts 3 weeks after they were injected with AAV9-shHMGA2 (1 week after the AB surgery) (n = 6, \*P < 0.05 vs. the AAV9-shRNA group). B. HW/BW, HW/TL, LW/BW, and LW/TL in mouse hearts 1 week after the AB surgery (n = 10). C. HE staining in the indicated groups (n = 6). D. Quantitative measurements of the cross-sectional areas of cardiomyocytes in the indicated groups (n = 100–200 left ventricular cells). E. Transcription of hypertrophic markers in the indicated mouse hearts (n = 6). F–I. Echocardiography and pressure volume loop were evaluated in mouse hearts after 1 week of AB (n = 8). F. Left ventricular end diastolic diameter (LVEDd), left ventricular end systolic diameter (LVESd), and left ventricular posterior wall diameter (LVPWd). G. Left ventricular ejection fraction (LVEF) and LV shortening fraction (LVFS). H. Heart rate, end systolic pressure (ESP), and end diastolic pressure (EDP). I. Cardiac output and left ventricular pressure maximal rate of rise and fall (dp/dtmax and dp/dtmin). \*P < 0.05 vs. the corresponding sham group; # P < 0.05 vs. the AAV9-shRNA-AB group.

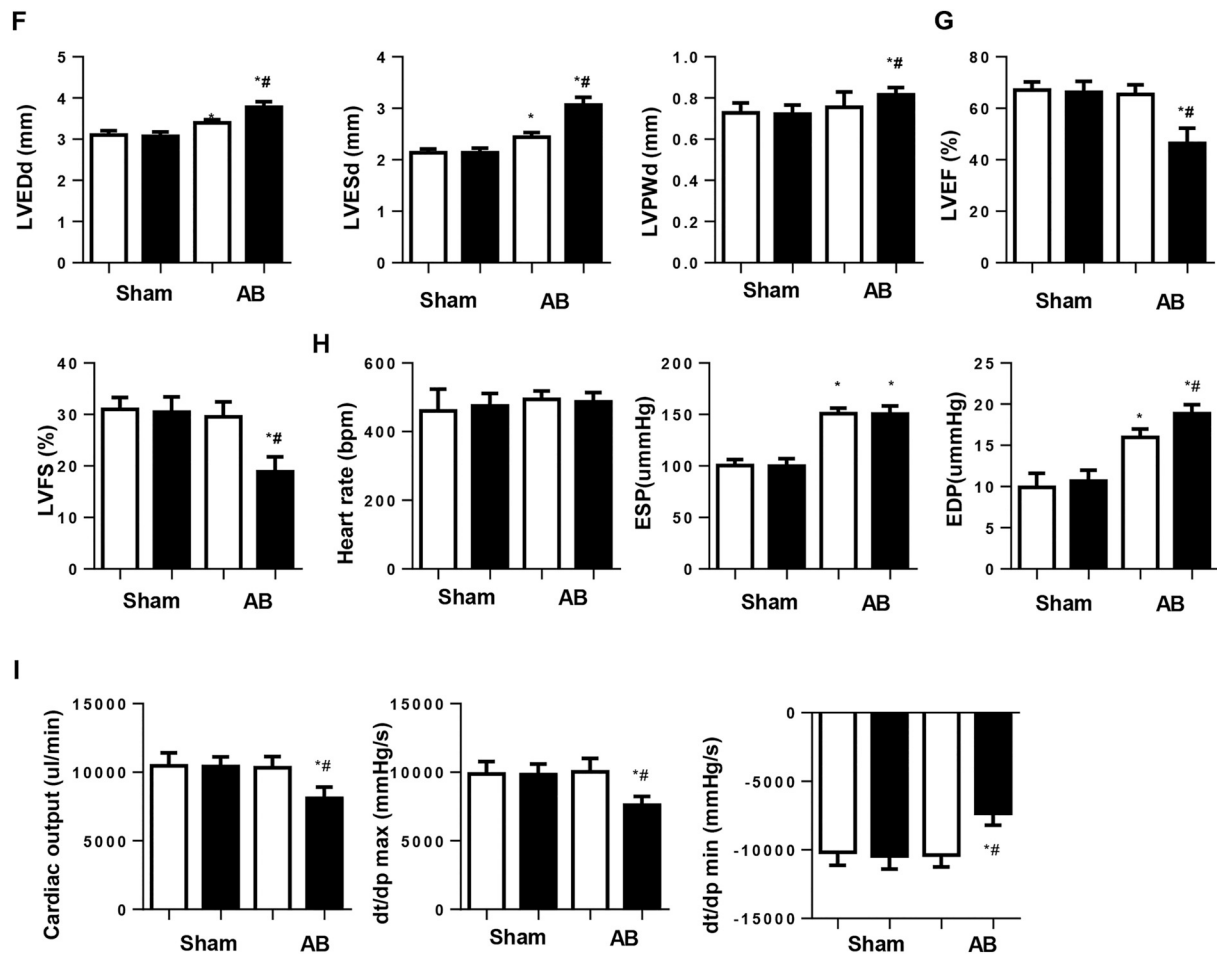


Fig. 5. (continued)

overload induced LV dilatation and thickening, as well as reduced systolic function. HMGA2 overexpression decreased LV end diastolic diameter (LVEDd) and the LV end systolic diameter (LVESd) (Fig. 4A), reduced the LV posterior wall diameter (LVPWd) (Fig. 4B), and increased the LV ejection fraction (LVEF) and LV shortening fraction (LVFS) (Fig. 4C). The heart rates in all four groups revealed no significant difference (Fig. 4D). The end systolic pressure (ESP) was not significantly different between the AAV9-HMGA2 and AAV9-NC groups after 8 weeks of AB (Fig. 4E). However, the end diastolic pressure (EDP) was decreased in the AAV9-HMGA2 group compared with that of the AAV9-NC group after 8 weeks of AB (Fig. 4E). Cardiac output and the LV pressure maximal rate of rise and fall (dp/dtmax and dp/dtmin) were increased in the AAV9-HMGA2 group compared with those of the AAV9-NC group after 8 weeks of AB (Fig. 4F–G). Interestingly, HMGA2 overexpression in the heart did not affect cardiac function under physiological conditions.

### 3.5. HMGA2 knockdown accelerates cardiac hypertrophy and dysfunction

Two weeks before the AB procedure, mice were randomly chosen to receive a heart injection of either AAV9-shHMGA2 or AAV9-shRNA (AAV9-NC) to knockdown HMGA2. Then, the mice were subjected to either aortic banding (AB) or a sham operation. After 1 weeks of AB, the mouse hearts were removed. As shown in Fig. 5, AAV9-shHMGA2 caused a decreased expression of HMGA2 1 week after the AB surgery

(Fig. 5A). Pressure overload induced increased HW/BW, HW/TL, LW/BW, and LW/TL ratios, and they were further increased in the HMGA2 knockdown group (Fig. 5B). Pressure overload induced an increased hypertrophic response (augmented cell surface area, transcription levels of hypertrophic markers) that was aggravated in the HMGA2 knockdown group. One week after the AB surgery, the mice showed increased LVEDd and LVESd values but no significant changes in LVPWd, LVEF or LVFS when compared with cardiac functions in sham mice. HMGA2 knockdown prevented the increase in LVEDd and LVESd, and it increased LVPWd and reduced LVEF and LVFS compared with the cardiac function of mice receiving the AAV9-shRNA injection (Fig. 5F–G). The pressure loop results demonstrated no significant differences in the heart rates among the four groups; pressure overload induced increases in ESP and EDP with no significant differences in cardiac output, dp/dt max, or dp/dt min, while HMGA2 knockdown further increased EDP and even reduced the cardiac output, dp/dt max, and dp/dt min after 1 weeks of AB when compared with the mice receiving an AAV9-shRNA injection (Fig. 5H, I). These data suggested that HMGA2 silencing accelerates pressure overload-induced cardiac remodeling and dysfunction.

### 3.6. HMGA2 overexpression inhibits oxidative stress in vivo and vitro

As oxidative stress plays a crucial role in cardiac remodeling process, we determined whether HMGA2 affects oxidative stress. HMGA2

overexpression increased superoxide dismutase (SOD) expression and activity, decreased NADPH oxidase P67 subunit expression and activity (Fig. 6A–D), and reduced lipid peroxide 4-hydroxynonenal (4-HNE) and malondialdehyde (MDA) levels (Fig. 6E, F) in mouse hearts in response to pressure overload.

We also detected the oxidative stress levels in PE-stimulated NRCMs. HMGA2 overexpression increased superoxide dismutase (SOD) expression and activity, decreased NADPH oxidase P67 and gp91 subunit expression and activity, and reduced reactive oxygen species (ROS) levels in cardiomyocytes (Fig. 6G–I). Together, these results demonstrate that HMGA2 may exert cardioprotection *via* regulating oxidative stress.

### 3.7. HMGA2 activates PPAR $\gamma$ /NRF2

Studies have reported that HMGA2 promotes adipogenesis *via* the activation of PPAR $\gamma$  in adipocytes [15]. Thus, we investigated the peroxisome proliferator-activated receptors, PPARs. As a result, we found that PPAR $\gamma$  was decreased 8 weeks after the AB surgery, while HMGA2 increased the PPAR $\gamma$  expression level (Fig. 7A). PPAR $\alpha$  was decreased and PPAR $\delta$  was increased 8 weeks after the AB surgery. HMGA2 overexpression did not affect the PPAR $\alpha$  or PPAR $\delta$  levels (Fig. 7A). We then measured the levels of the downstream molecules keap, PGC1 $\alpha$ , and NRF2. Overexpression HMGA2 increased the expression levels of keap, PGC1 $\alpha$ , and NRF2 in heart tissue 8 weeks after

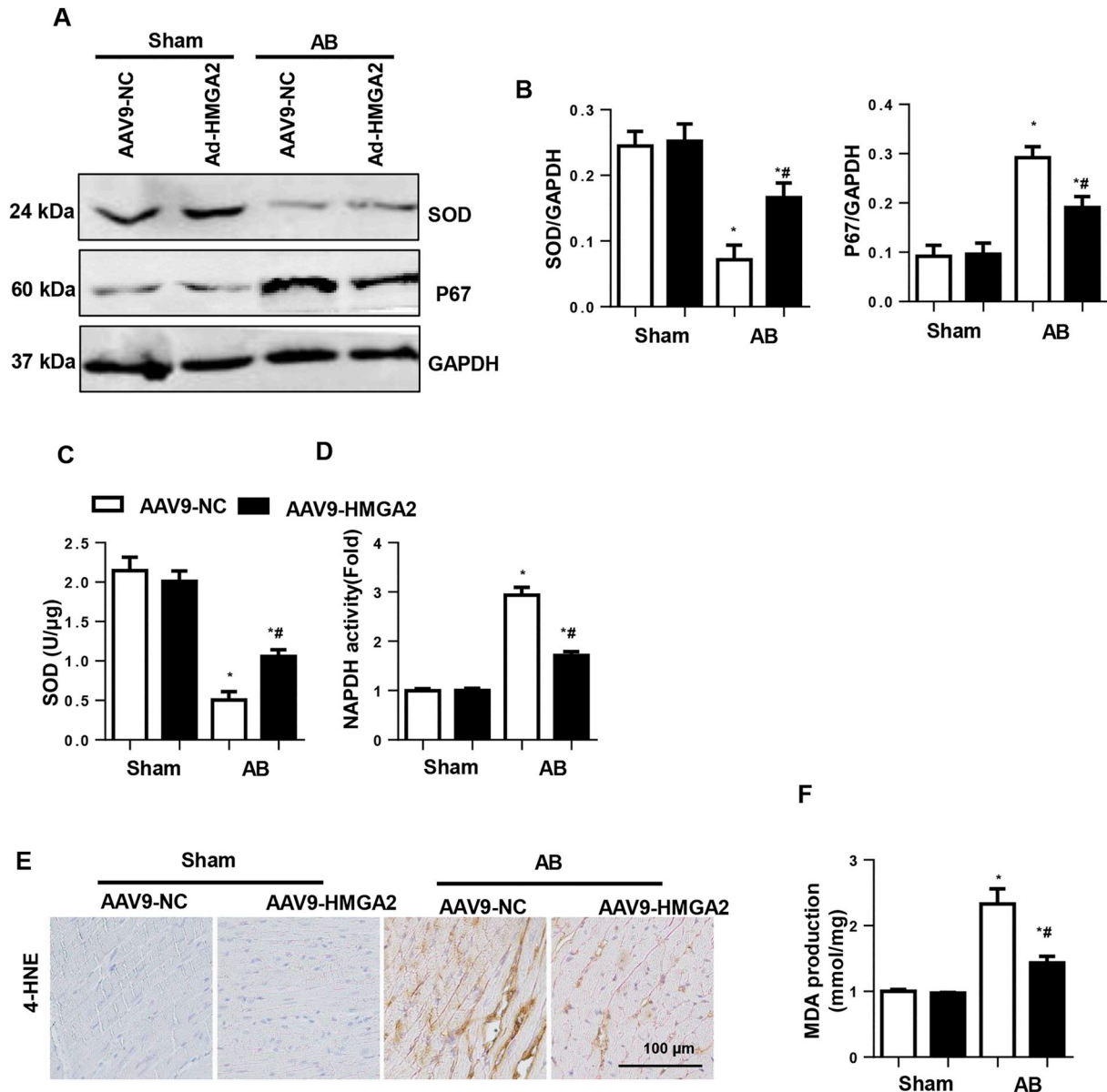


Fig. 6. HMGA2 overexpression inhibits oxidative stress *in vivo* and *in vitro*.

A and B. Protein expression levels of SOD and P67 in mouse hearts 8 weeks after the AB surgery in the indicated groups (n = 6). C and D. SOD and NADPH oxidase activities in the indicated groups (n = 6). E. Immunohistochemical staining for 4-hydroxynonenal (4-HNE) in the mouse hearts in the indicated groups. F. MDA production in the indicated mouse hearts. \*P < 0.05 vs. the corresponding sham group; # P < 0.05 vs. the AAV9-NC-AB group.

G and H. Protein expression levels of SOD, P67, and gp91 in cardiomyocytes that were transfected with Ad-HMGA2 and stimulated with PE for 48 h (n = 6). I. ROS level and SOD and NADPH oxidase activities in the indicated groups (n = 6). \*P < 0.05 vs. the corresponding control group; # P < 0.05 vs. the Ad-NC-PE group.

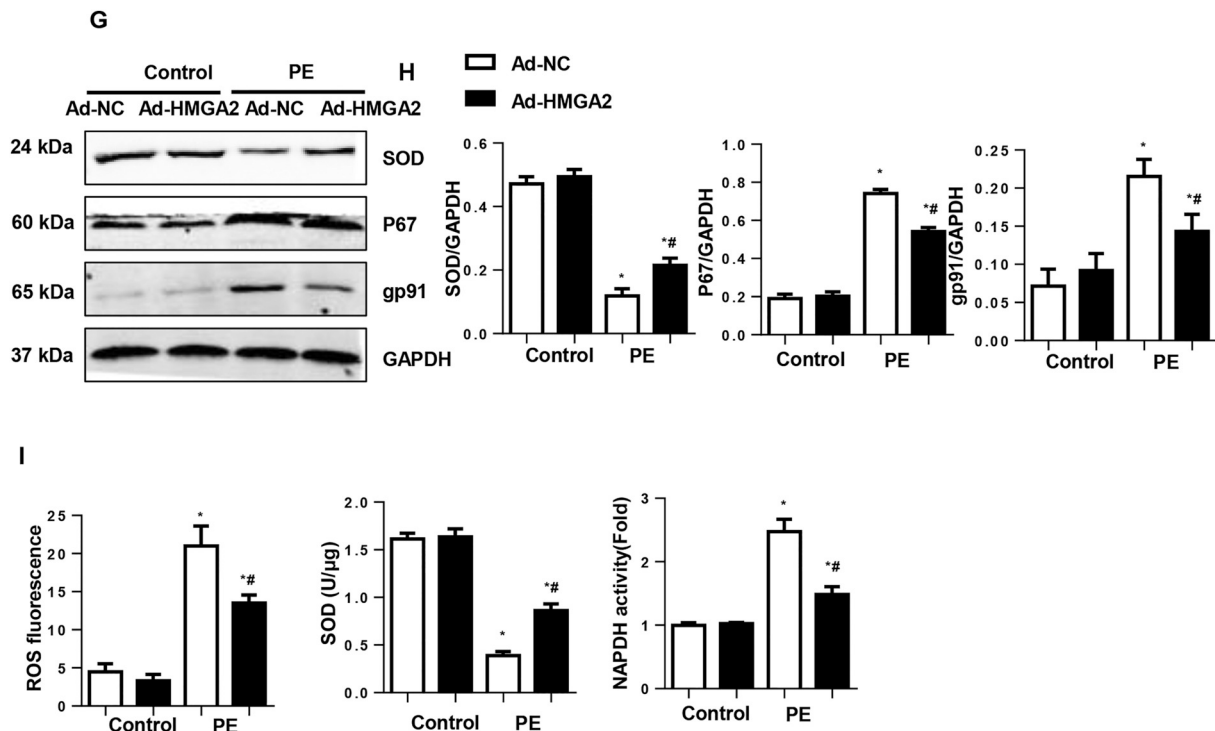


Fig. 6. (continued)

the AB surgery, and it also increased NRF2 nuclear transition in response to pressure overload (Fig. 7C, D). We confirmed these alterations with an *in vitro* study, and we consistently found that HMGA2 overexpression in NRCMs increased PPAR $\gamma$  and NRF2 expression as well as NRF2 nuclear transition in response to PE stimuli (Fig. 7E, F). We then supposed that the activation of PPAR $\gamma$  may be due to the direct interaction of HMGA2 with PPAR $\gamma$ . We unexpectedly found that the HMGA2 protein did not interact with PPAR $\gamma$  (Fig. 7G). Since HMGA2 is a transcription factor, we then determined whether HMGA2 regulates PPAR $\gamma$  transcription. We performed a reporter assay using a luciferase gene under the control of the PPAR $\gamma$  promoter. As displayed in Fig. 6H, neither overexpression nor knockdown of HMGA2 affected the reporter expression. Our results strongly suggested that other mechanisms may mediate the effect of HMGA2 on PPAR $\gamma$ .

### 3.8. PPAR $\gamma$ inhibition offsets the protective effect of HMGA2 *in vitro*

We then explored the significance of PPAR $\gamma$ /NRF2 on HMGA2-mediated cardioprotection. NRCMs were transfected with Ad-HMGA2 and then stimulated with PE and treated with GW9962 for 48 h. As expected, the PPAR $\gamma$  inhibitor GW9962 offset the antihypertrophic (Fig. 8A, B) and antioxidative stress (Fig. 8C) responses of HMGA2. The NRCMs were then treated with siHMGA2 and stimulated with PE for 24 h, and they were then treated with PPAR $\gamma$  activator rosiglitazone (BRL49653, 1  $\mu$ M) for 2 h. The HMGA2 silencing-induced deterioration of cardiomyocyte remodeling was relieved by BRL49653, as accessed by the decreased cell surface area, reduced transcription levels of hypertrophic markers and reduced oxidative stress in BRL49653-treated cells compared with those of siHMGA2 + PE-treated cells (Fig. 8D–F).

We then used NRF2 siRNA to knock down NRF2 (Fig. 8G). As a result, NRF2 silencing also abolished the antihypertrophic (Fig. 8H, I) and antioxidative stress (Fig. 8J) responses of HMGA2. These data

directly indicate that HMGA2 exerts cardioprotection mainly via PPAR $\gamma$ /NRF2 signaling.

### 3.9. PPAR $\gamma$ knockdown abolished the cardioprotection properties of HMGA2 *in vivo*

To confirm the cause and effect of HMGA2-mediated cardioprotection, mice were subjected to AAV9-shPPAR $\gamma$  to knock down PPAR $\gamma$  (Fig. 9A). Mice with PPAR $\gamma$  knockdown showed deteriorating cardiac remodeling and dysfunction as evidenced by their increased HW/BW, HW/TL, LW/BW, and LW/TL ratios, increased cell surface area, LV collagen volume, increased LVEDd, LVESd, and LVPWd, reduced LVEF and LVFS and decreased dp/dtmax and dp/dtmin when compared with mice in the AAV9-NC group 4 weeks after the AB surgery (Fig. 9B–H). After 4 weeks of AB, we found that the hypertrophic response (Fig. 9B–D) and the extent of fibrosis (Fig. 9E, F) resulting from pressure overload were not significantly different between the AAV9-shPPAR $\gamma$  group and the AAV9-shPPAR $\gamma$  + AAV9-HMGA2 group. Moreover, the cardiac dysfunction in response to pressure overload was not significantly different between the AAV9-shPPAR $\gamma$  group and AAV9-shPPAR $\gamma$  + AAV9-HMGA2 group (Fig. 9G, H). These data confirm our hypothesis that HMGA2 protects against pressure overload-induced cardiac remodeling via regulating PPAR $\gamma$  expression.

### 3.10. The interaction of HMGA2 with C/EBP $\beta$ mediated the transcriptional regulation of PPAR $\gamma$ expression

One study reported that HMGA2 interacted with C/EBP $\beta$ , which was recruited to the binding element at the PPAR $\gamma$  promoter in adipocytes [15]. We used C/EBP $\beta$  siRNA to knock down C/EBP $\beta$  (Fig. 10A) and found that the HMGA2 overexpression-induced increase in PPAR $\gamma$  expression was reduced by C/EBP $\beta$  silencing (Fig. 10B). A co-IP study

found that HMGA2 interacted with the C/EBP $\beta$  protein in cardiomyocytes (Fig. 10C). The endogenous interaction of HMGA2 and C/EBP $\beta$  was confirmed by using mouse heart extracts at 1 week post AB. Consistent with the *in vitro* result, HMGA2 interacted with C/EBP $\beta$  in mouse heart extracts (Fig. 10D). C/EBP $\beta$  overexpression increased the expression of the PPAR $\gamma$  reporter, and HMGA2 further increased the PPAR $\gamma$  promoter activity in C/EBP $\beta$ -overexpressing 293 T cell lines (Fig. 10E). Studies have proven that C/EBP $\beta$  exerts an essential role in exercise-induced cardiac hypertrophy and that C/EBP $\beta$  regulates the upregulation of hypertrophy-related genes such as Gata4, Tbx5, Nkx2.5, TnT, and TnI [16]. To confirm whether HMGA2 affected other downstream factors that contribute to hypertrophy, cells were treated with HMGA2 siRNA and Ad-C/EBP $\beta$ . As shown in Fig. 10F, HMGA2 silencing did not affect the transcription level of Gata4, Tbx5, Nkx2.5, or TnT, but C/EBP $\beta$  overexpression reduced the transcription levels of these prohypertrophic factors. The transcription levels of these prohypertrophic factors were not significantly difference between cells

treated with Ad-C/EBP $\beta$  and cells treated with both Ad-C/EBP $\beta$  and HMGA2 siRNA. These findings indicate that another downstream factor of C/EBP $\beta$  is not the target of HMGA2.

NRCMs were treated with C/EBP $\beta$  siRNA and stimulated with PE. The cardioprotection of HMGA2 overexpression was abolished by C/EBP $\beta$  knockdown (Fig. 10G–I). This finding strongly suggests that HMGA2 interacts with C/EBP $\beta$  to regulate the expression of PPAR $\gamma$ , thus protecting cardiac remodeling.

#### 4. Discussion

Here, we revealed that HMGA2 plays a previously unrecognized role in pressure overload-induced cardiac remodeling. Our results suggested that HMGA2 has a protective effect against pressure overload-induced cardiac hypertrophy and fibrosis and improves cardiac function. HMGA2 blocked myocardial ROS production and oxidative stress induced by long-term pressure overload. The cardioprotective effects of

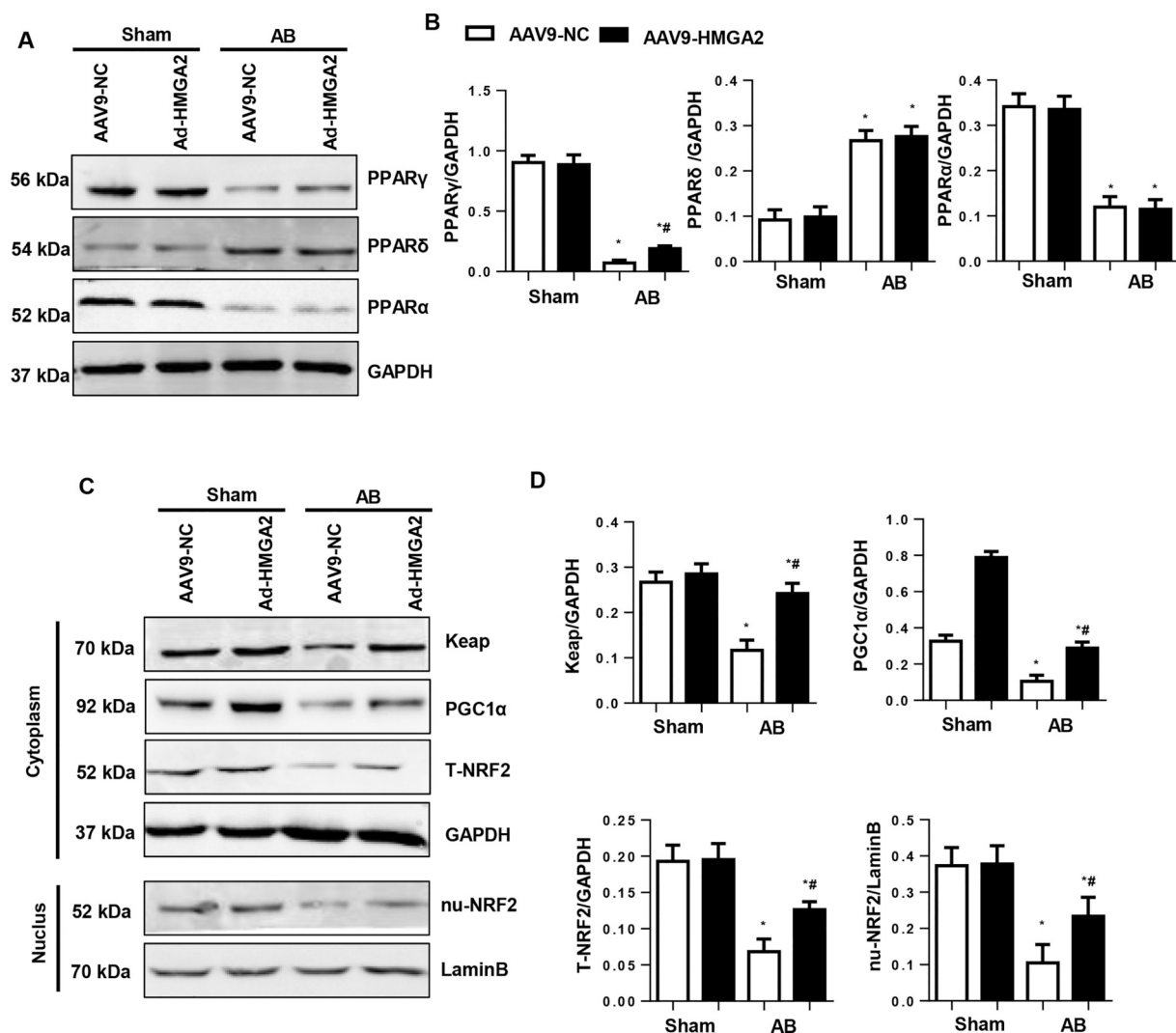


Fig. 7. HMGA2 activates PPAR $\gamma$ /NRF2.

A and B. The protein expression levels of PPAR $\gamma$ , PPAR $\alpha$ , and PPAR $\delta$  in mouse hearts 8 weeks after the AB surgery (n = 6). C and D. The protein expression levels of keap1, PGC1 $\alpha$ , and NRF2 in mouse hearts 8 weeks after the AB surgery (n = 6). \*P < 0.05 vs. the corresponding sham group; # P < 0.05 vs. the AAV9-NC-AB group. E and F. The protein expression levels of PPAR $\gamma$  and NRF2 in cardiomyocytes that were transfected with Ad-HMGA2 and stimulated with PE for 48 h (n = 6). \*P < 0.05 vs. the corresponding control group; # P < 0.05 vs. the Ad-NC-PE group. G. Coimmunoprecipitation experiments showing the physical interactions between HMGA2 and PPAR $\gamma$  in cardiomyocytes. H. Relative luciferase activity of the PPRE promoter in HEK293T cells.

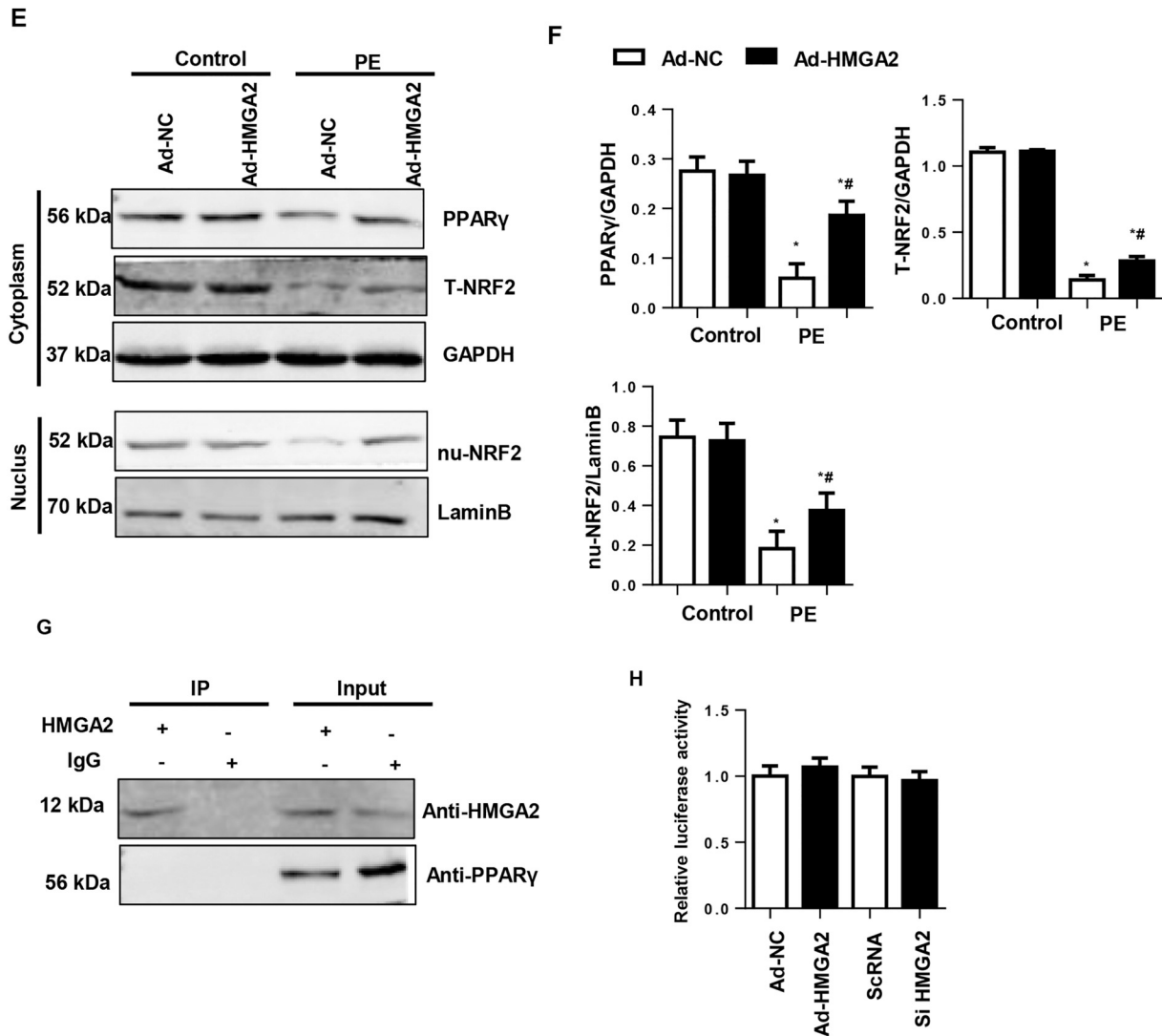


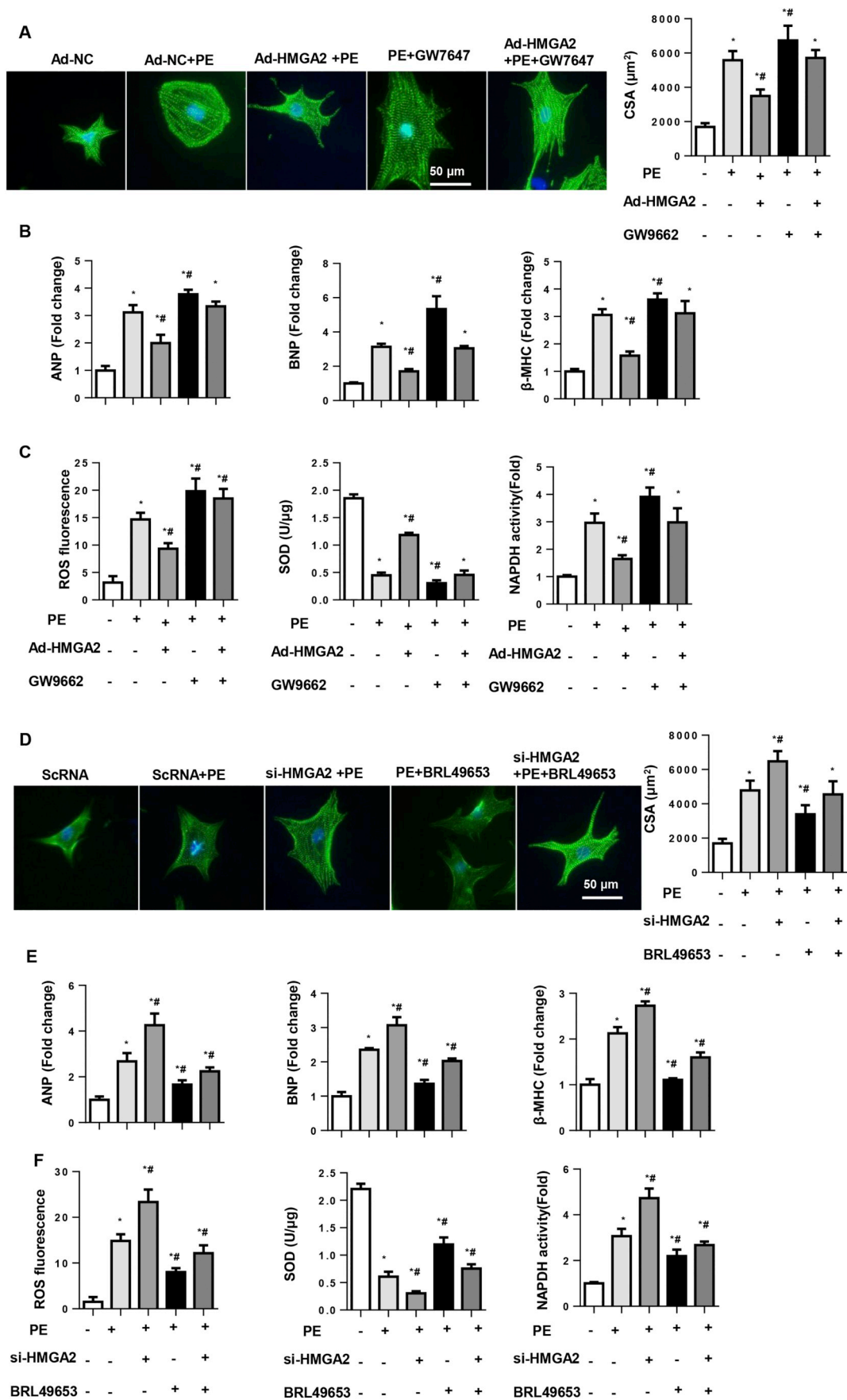
Fig. 7. (continued)

HMGA2 were mediated by PPAR $\gamma$ /NRF2, which were activated *via* binding to C/EBP $\beta$ . Knocking down PPAR $\gamma$  *in vivo* and *in vitro* completely abolished the protective effects of HMGA2. Knocking down C/EBP $\beta$  in cardiomyocytes also offset HMGA2-mediated effects in cardiomyocytes.

HMGA2 encodes a member of the HMGA family of proteins and is implicated in chromatin remodeling and regulation of transcription. It is overexpressed in many human solid tumors, and its upregulation was thought to be potentially associated with tumor progression and a poor prognosis [6]. Previous studies have reported that HMGA2 is expressed ubiquitously during embryogenesis and has low expression levels in fully differentiated adult tissues [15]. HMGA2 was found to play a critical function in cardiogenesis during embryogenesis, and the knockdown of HMGA2 expression blocked normal heart formation in *Xenopus laevis* embryos [5]. In this study, we found that during the pathology of cardiac remodeling, HMGA2 was upregulated in the early stage of the remodeling heart and cardiomyocytes and it then dropped rapidly in the later remodeling processes. These findings indicate that HMGA2 participates in the remodeling process during cardiac insult. Our data clearly demonstrated that HMGA2 overexpression ameliorated cardiac dysfunction by attenuating cardiac hypertrophy and cardiac

fibrosis in mice undergoing cardiac remodeling. Furthermore, HMGA2 knockdown during the early stage (24 h) of PE stimulation caused a deterioration in the hypertrophic response to PE.

PPARs are nutrient sensors that regulate a number of homeostatic functions. Three isoforms of nuclear receptors have been discovered: PPAR $\alpha$ , PPAR $\delta$  and PPAR $\gamma$  [17]. PPARs participate in the regulation of cell growth, migration and apoptosis, and they may modulate oxidative stress, antioxidant responses and inflammatory diseases in the cardiovascular system [17,18]. Disruptions of PPAR pathways can result in the development of several diseases and pathological states, such as atherosclerosis, diabetes mellitus, metabolic syndrome and hypertension [19–21]. A previous study found that HMGA2 regulated PPAR $\gamma$  expression in adipocytes [15]. In our study, we found that the expression of PPAR $\alpha$  was decreased and PPAR $\delta$  was increased in the remodeling mouse hearts. However, both PPAR $\alpha$  and PPAR $\delta$  were not affected in the HMGA2-overexpressing hearts. Only PPAR $\gamma$  was decreased in the remodeling mouse hearts, and it was upregulated by HMGA2 overexpression. We also found that HMGA2 increased the promoter activity of PPAR $\gamma$ . Ira Goldberg's group has reported that PPAR $\gamma$ 1 transgenic mice developed a dilated cardiomyopathy that was



(caption on next page)

**Fig. 8.** PPAR $\gamma$  inhibition offset the protective effect of HMGA2 *in vitro*.

A-C. NRCMs were transfected with Ad-HMGA2 then stimulated with PE for 48 h and treated with the PPAR $\gamma$  inhibitor GW9662 (10  $\mu$ M). A.  $\alpha$ -actin staining and quantitative results for the detection of the cell surface areas in the indicated groups (n > 50 cells per group). B. Transcription of hypertrophic markers in the indicated groups (n = 6). C. ROS level and SOD and NADPH oxidase activities in the indicated groups (n = 6). \*P < 0.05 vs. the Ad-NC group; # P < 0.05 vs. the Ad-NC + PE group.

D-F. NRCMs were treated with siHMGA2 and stimulated with PE for 24 h then treated with the PPAR $\gamma$  activator rosiglitazone (BRL49653, 1  $\mu$ M) for 2 h. D.  $\alpha$ -actin staining and quantitative results (n > 50 cells per group). E. Transcription of hypertrophic markers (n = 6). F. ROS levels and SOD and NADPH oxidase activities (n = 6). \*P < 0.05 vs. the ScrNA group; # P < 0.05 vs. the ScrNA + PE group.

G-J. NRCMs were transfected with Ad-HMGA2, treated with NRF2 siRNA, and then stimulated with PE for 48 h. G. Expression level of NRF2 in NRCMs after treatment with NRF2 siRNA. H and G.  $\alpha$ -actin staining (F) and quantitative results (G) for the detection of cell surface area in the indicated groups (n > 50 cells per group). I. Transcription of hypertrophic markers in the indicated groups (n = 6). J. ROS levels and SOD and NADPH oxidase activities in the indicated groups (n = 6). \*P < 0.05 vs. the Ad-NC group; # P < 0.05 vs. the Ad-NC + PE group.

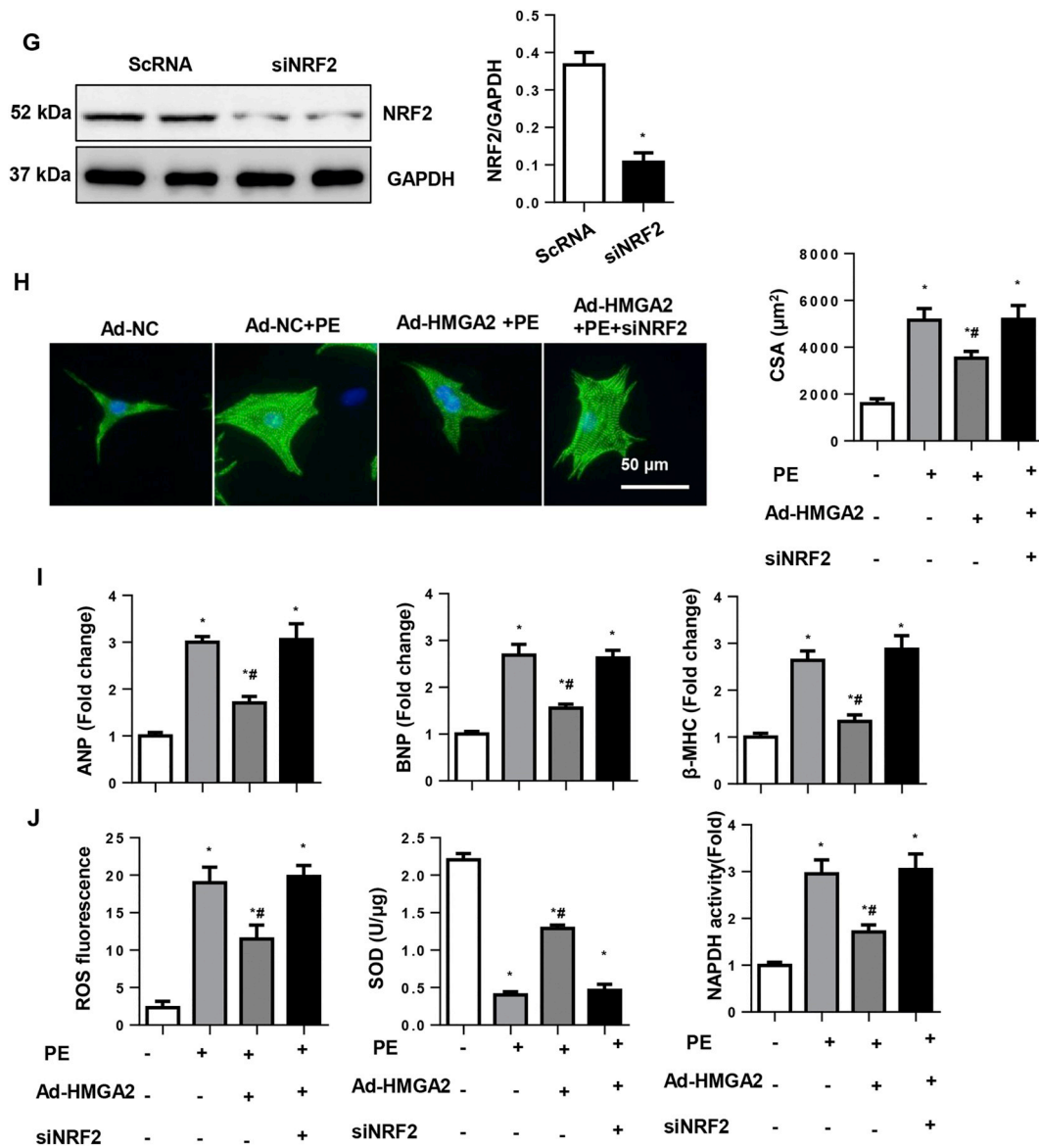


**Fig. 8.** (continued)

associated with increased lipid and glycogen storage, distorted architecture of the mitochondrial inner matrix, and disrupted cristae in aging mice [22]. However, Duan SZ's study found that cardiomyocyte PPAR $\gamma$  suppresses cardiac growth and embryonic gene expression and inhibits

nuclear factor kappa B activity [23]. Asakawa M's study revealed that PPAR $\gamma$  ligands such as troglitazone, pioglitazone, and rosiglitazone inhibited Ang II-induced cardiomyocyte hypertrophy and inhibited pressure overload-induced cardiac hypertrophy [24]. These results

show that the role of PPAR $\gamma$  in the heart has been controversial. However, the  $\alpha$ -MHC-PPAR $\gamma$  transgene mice in Ira Goldberg's study may have a much higher relative expression of PPAR $\gamma$ , thus leading to the accumulation of fatty acids and cardioliptotoxicity. In our study, we found that PPAR $\gamma$  knockdown in mouse hearts caused an increased hypertrophic response, which indicates the protective role of PPAR $\gamma$  in pressure overload-induced cardiac hypertrophy. Ira Goldberg also

reported that PPAR $\gamma$ -induced cardioliptotoxicity is ameliorated by PPAR $\alpha$  deficiency [25]. They believe that both PPAR $\alpha$  and PPAR $\gamma$  increase lipid uptake and have overlapping functions in metabolic heart disease. Additionally, the beneficial phenotype that they observed was attributed to PPAR $\alpha$  and PPAR $\gamma$  inhibition in metabolic disorders. However, in pressure overload-induced cardiac hypertrophy, the metabolic changes involved reduced oxidative metabolism, whereas

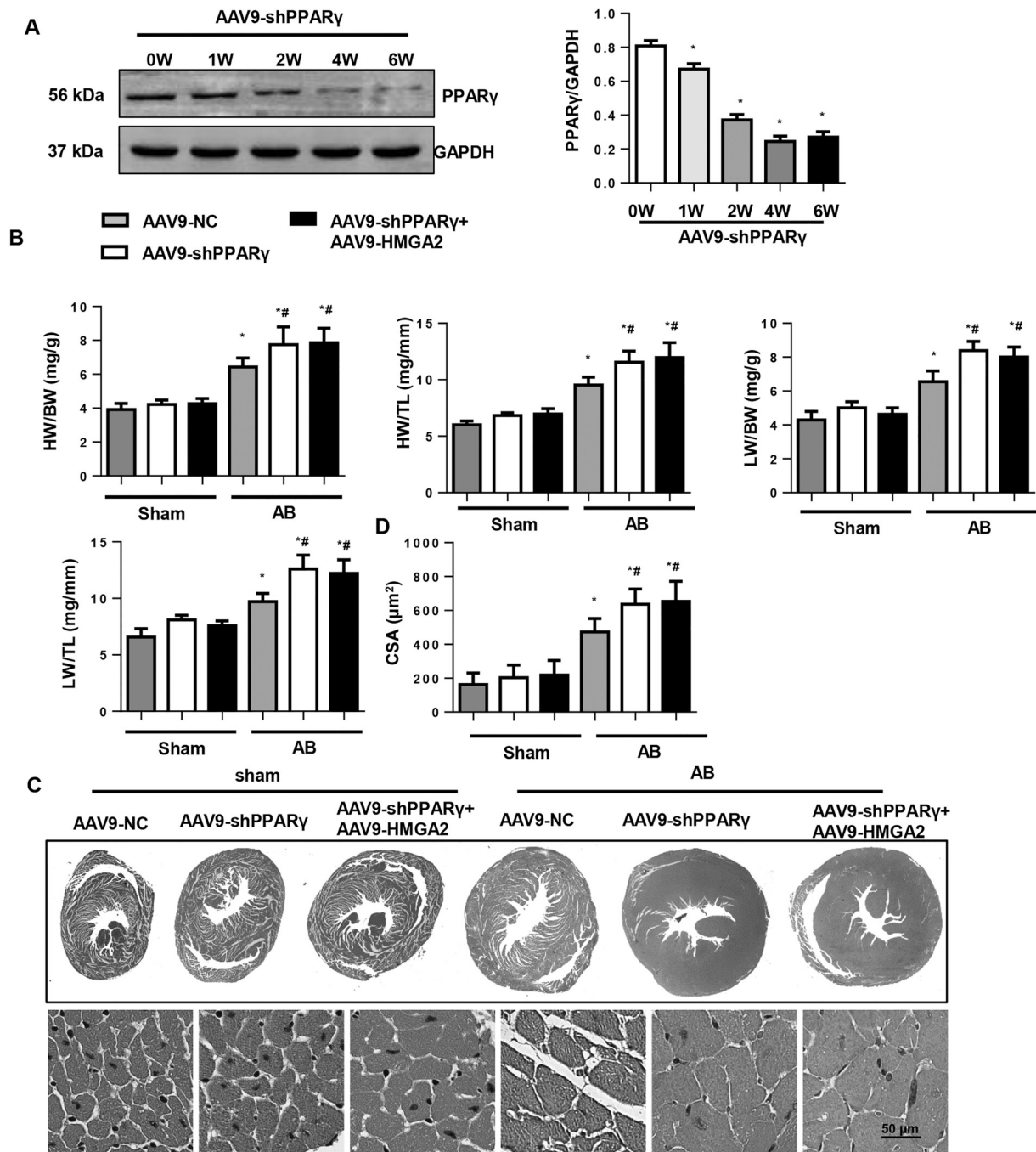


**Fig. 9.** PPAR $\gamma$  knockdown abolished the cardioprotective effects of HMGA2 *in vivo*.

A. PPAR $\gamma$  protein expression level in mouse hearts at 0, 1, 2, 4, 6 weeks after mice were injected with AAV9-shPPAR $\gamma$  (n = 6, \*P < 0.05 vs. the AAV9-shRNA group). B. HW/BW, HW/TL, LW/BW, and LW/TL in mouse hearts 8 weeks after the AB surgery (n = 10). C. HE staining in the indicated groups (n = 6). D. Quantitative measurements of the cross-sectional area of cardiomyocytes in the indicated groups (n = 100–200 left ventricular cells). E. PSR staining to detect collagen accumulation (n = 6). F. Quantitative results of the left ventricular collagen volume in the indicated groups (n = 6). G and H. Echocardiography and pressure volume loop were evaluated in mouse hearts after 8 weeks of AB (n = 8). \*P < 0.05 vs. the corresponding sham group; #P < 0.05 vs. the AAV9-NC-AB group.

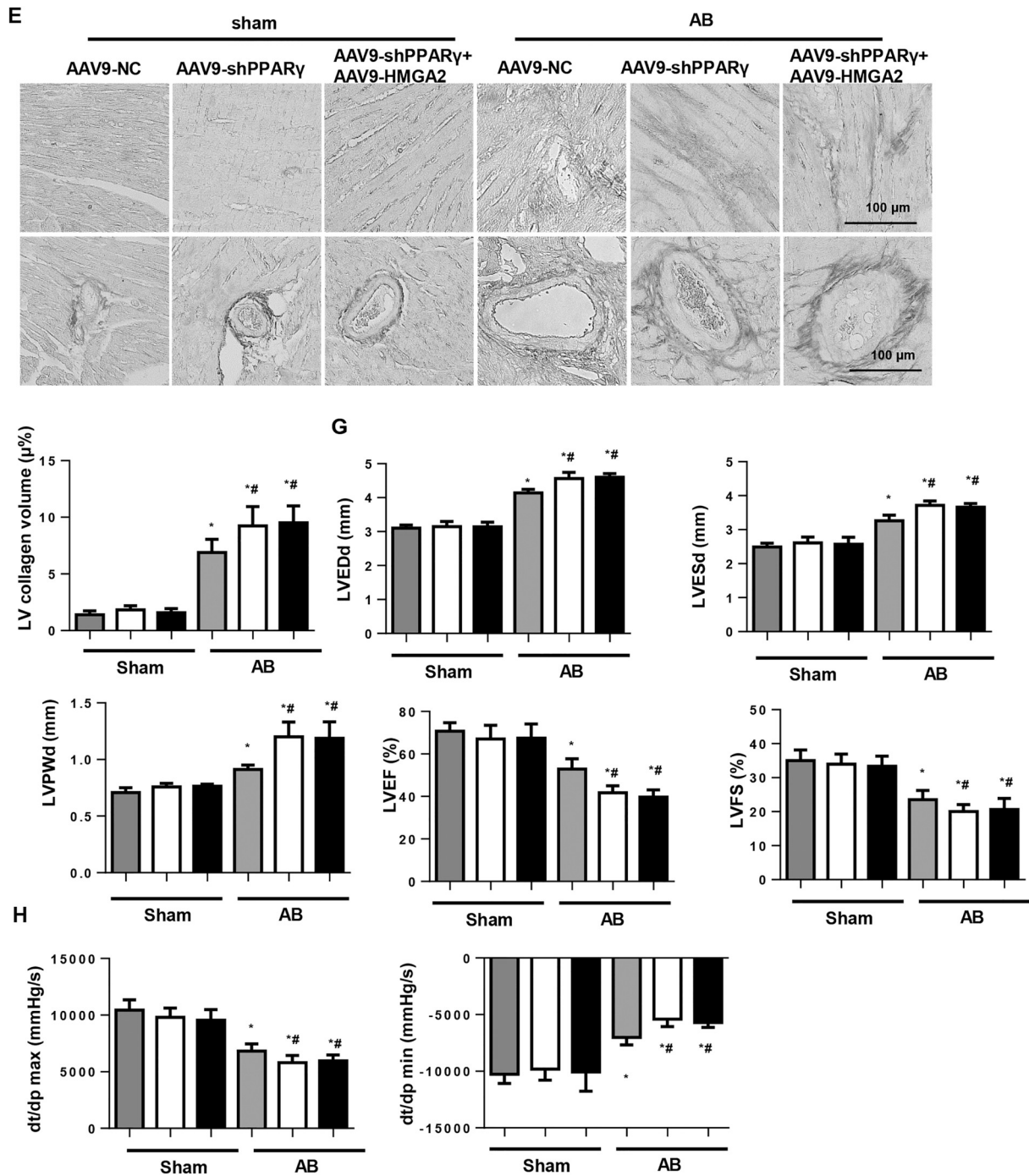


Fig. 9. (continued)

diabetic cardiomyopathy resulted in an increase in fatty acid oxidation due to increased circulating levels of fatty acids. In the hypertrophic failing heart, glycolysis is increased and as fatty acid and glucose oxidation are suppressed, *i.e.*, cardiac metabolism reverts back to the “fetal phase” [26]. Thus, increasing PPAR $\gamma$  could improve metabolic changes and benefit the heart [27]. In our study, we showed the benefit of PPAR $\gamma$  activation, and these benefits do not rely upon the secondary alteration of PPAR $\alpha$  since we did not observe any changes in the PPAR $\alpha$  levels after HMGA2 overexpression or knockdown.

The Keap1/Nrf2/ARE pathway is a complex system maintaining redox homeostasis in normal or stress conditions [28]. During oxidative

stress, Nrf2 can be released from its connection with Keap1 and is translocated to the nucleus, where it induces the transcription of genes by AREs, which then target the transcription of genes that are directly involved in the production of antioxidant and detoxification proteins [29,30]. PPAR $\gamma$  can act directly or through an upstream pathway for Nrf2 activation [18]. In our study, we found that the excessive oxidative stress in the remodeling heart was suppressed by HMGA2 overexpression. These responses contribute to the activation of PPAR $\gamma$  since PPAR $\gamma$  inhibition/knockdown or NRF2 knockdown totally abolished the cardioprotective effect of HMGA2 overexpression.

Evidence suggests that C/EBP $\beta$  plays a vital role in regulating

PPAR $\gamma$  transcription during adipogenesis [31] and ischemic stroke [18]. Studies have reported that HMGA2 enhances the C/EBP $\beta$ -mediated transcription of the PPAR $\gamma$  gene in adipocytes [15]. With our data, we support the hypothesis that HMGA2 interacts with C/EBP $\beta$  to regulate the transcription of the PPAR $\gamma$  gene in cardiomyocytes. The HMGA2 overexpression-mediated PPAR $\gamma$  promoter activation was reliant upon

C/EBP $\beta$ . Moreover, C/EBP $\beta$  knockdown also blunted the protective effect of HMGA2 on cardiomyocyte hypertrophy and oxidative stress. Studies have proven that C/EBP $\beta$  exerts an essential role in exercise-induced cardiac hypertrophy; C/EBP $\beta$  regulates the upregulation of hypertrophy-related genes such as Gata4, Tbx5, Nkx2.5, TnT, and TnI [16]. However, in our study we observed a negative effect of HMGA2

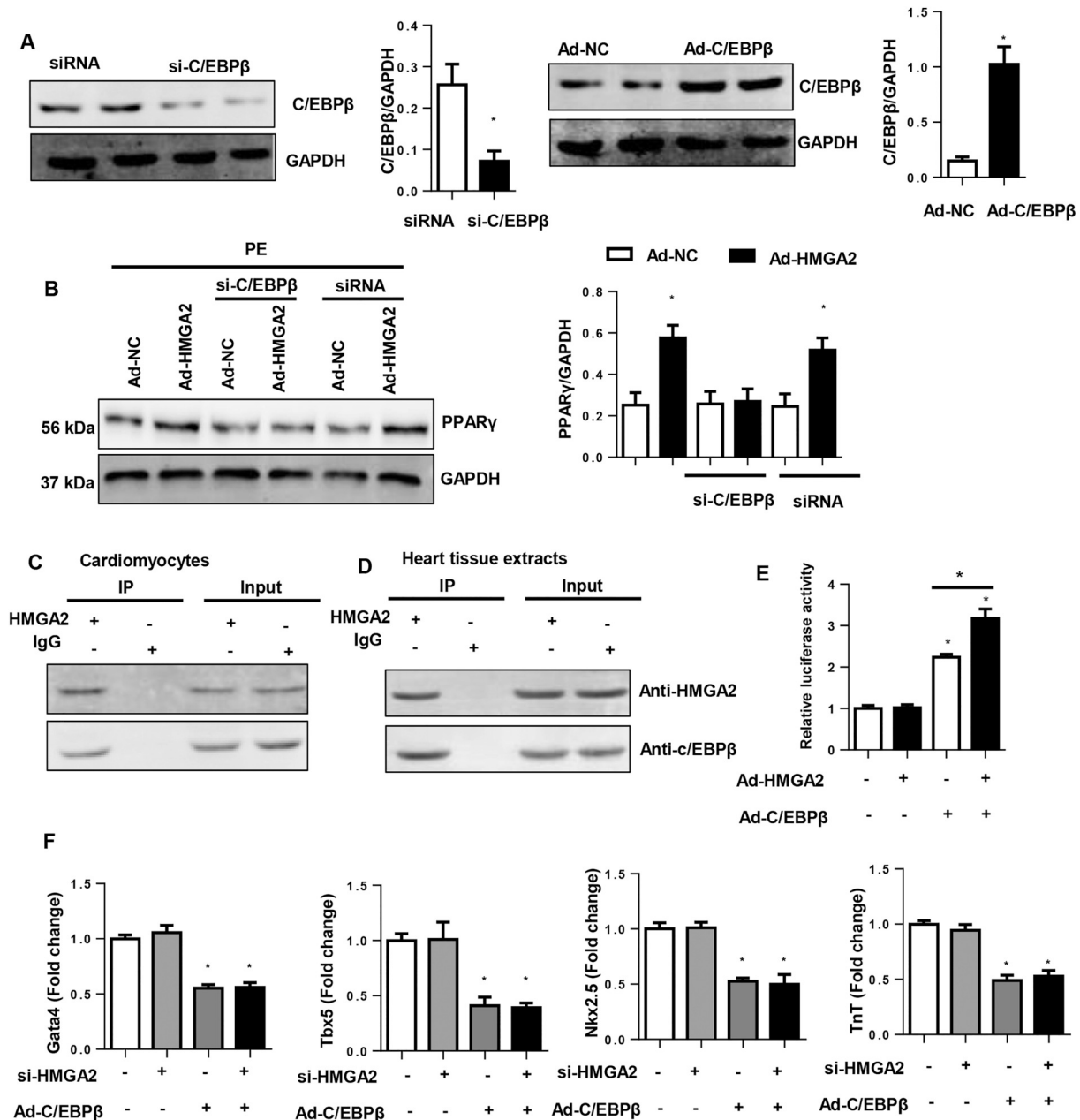
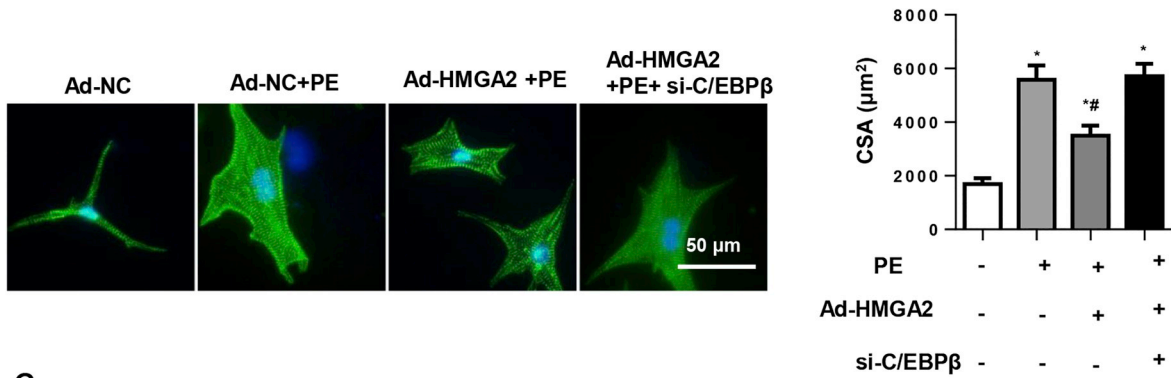


**Fig. 10.** HMGA2 interacted with C/EBP $\beta$  to mediate the transcriptional regulation of PPAR $\gamma$  expression.

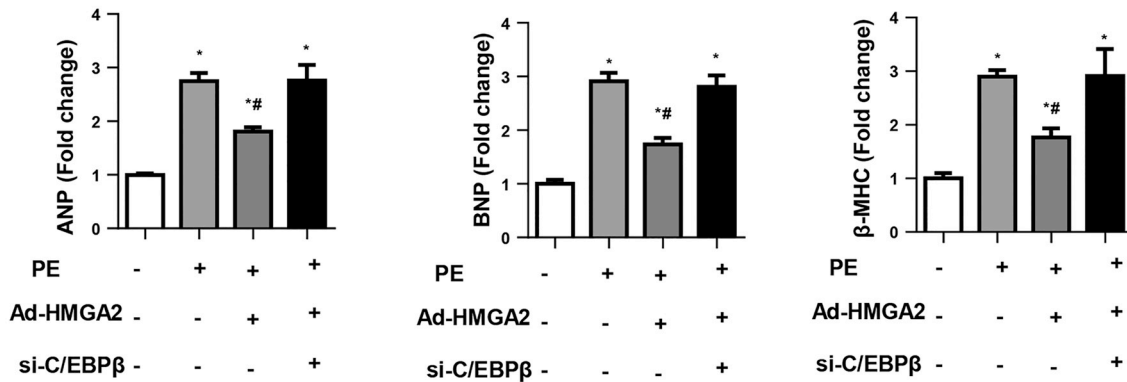
A. NRCMs were transfected with C/EBP $\beta$  siRNA. The expression levels of C/EBP $\beta$  (n = 6). B. NRCMs were transfected with Ad-HMGA2 and C/EBP $\beta$  siRNA and then stimulated with PE. The expression level of PPAR $\gamma$  (n = 6). C. Coimmunoprecipitation experiments showing the physical interactions between HMGA2 and C/EBP $\beta$  in cardiomyocytes. D. Coimmunoprecipitation experiments showing the endogenous interactions between HMGA2 and C/EBP $\beta$  in heart tissue extracts 1 week post AB surgery. E. Relative luciferase activity of the PPRE promoter in HEK293 cells that were transfected with Ad-C/EBP $\beta$  or Ad-HMGA2 (\*P < 0.05 vs. the Ad-NC group). F. NRCMs were transfected with Ad-C/EBP $\beta$  and/or HMGA2 siRNA. The transcription of Gata4, Tbx5, Nkx2.5, and TnT (n = 6, \*P < 0.05 vs. the control group).

G–I. NRCMs were transfected with Ad-HMGA2 and treated with C/EBP $\beta$  siRNA. G.  $\alpha$ -actin staining and quantitative results for the detection of cell surface areas in the indicated groups (n > 50 cells per group). H. Transcription of hypertrophic markers in the indicated groups (n = 6). I. ROS levels and SOD and NADPH oxidase activities in the indicated groups (n = 6). \*P < 0.05 vs. the Ad-NC group; # P < 0.05 vs. the Ad-NC + PE group.

F



G



H

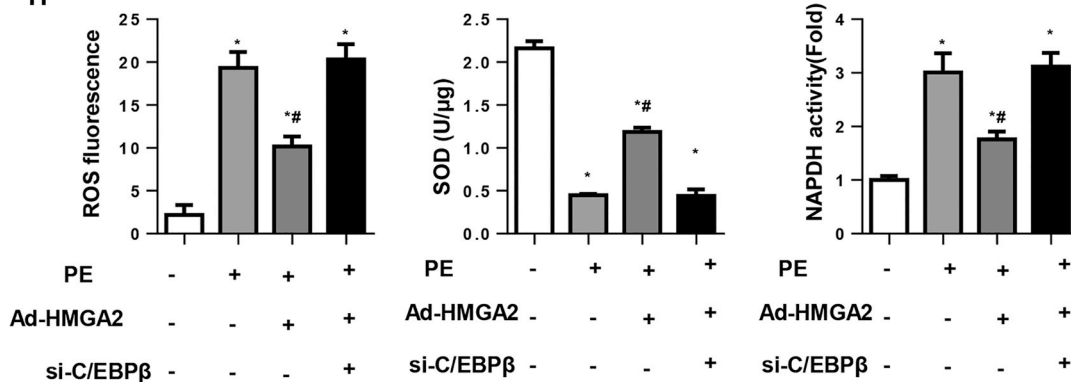


Fig. 10. (continued)

on Gata4, Tbx5, Nkx2.5, and TnT transcription. One study reported that C/EBPβ interferes with serum response factor (SRF) binding to the promoters of these critical cardiac genes (including Gata4, Tbx5, and Nkx2.5) [32]. Our negative result indicates that HMGA2 binding to C/EBPβ merely regulates PPARγ signaling and no other signaling such as that of SRF, thus regulating cardiac hypertrophy under stress.

In conclusion, we found that HMGA2 ameliorated pressure overload-induced cardiac remodeling by promoting PPARγ expression. Our study has provided basic evidence for the targeting of HMGA2 in the treatment of cardiac remodeling and heart failure.

**Conflict of interests**

The authors declare no conflicts of interest.

**Authors' contribution**

Qing-Qing Wu and Qi-Zhu Tang contributed to the conception and design of the experiments; Qing-Qing Wu, Yang Xiao, Chen Liu, and Ming-Xia Duan carried out the experiments; Zhulan Cai and Saiyang Xie analysed the experimental results and revised the manuscript; Wei Deng, Haiming Wu and Yuan Yuan wrote and revised the manuscript.

**Sources of funding**

This work was supported by grants from the National Natural Science Foundation of China (No. 81470516, 81530012, 81700353) and Fundamental Research Funds of the Central Universities (2042017kf0060).

## References

- [1] Q.Q. Wu, Y. Xiao, Y. Yuan, Z.G. Ma, H.H. Liao, C. Liu, J.X. Zhu, Z. Yang, W. Deng, Q.Z. Tang, Mechanisms contributing to cardiac remodelling, *Clin. Sci. (Lond)* 131 (18) (2017) 2319–2345.
- [2] Z.K. Haque, D. Wang, How cardiomyocytes sense pathophysiological stresses for cardiac remodeling, *Cell. Mol. Life Sci.* 74 (6) (2017) 983–1000.
- [3] M. Hou, X. Bao, F. Luo, X. Chen, L. Liu, M. Wu, HMGA2 modulates the TGFβ/Smad, TGFβ/ERK and notch signaling pathways in human lens epithelial-mesenchymal transition, *Curr. Mol. Med.* 18 (2) (2018) 71–82 (Epub ahead of print).
- [4] S. Zhang, Z. Huibian, L. Yu, HMGA2 promotes glioma invasion and poor prognosis via a long-range chromatin interaction, *Cancer Med.* (2018) (Epub ahead of print).
- [5] K. Monzen, Y. Ito, A.T. Naito, H. Kasai, Y. Hiroi, D. Hayashi, I. Shiojima, T. Yamazaki, K. Miyazono, M. Asashima, R. Nagai, I. Komuro, A crucial role of a high mobility group protein HMGA2 in cardiogenesis, *Nat. Cell Biol.* 10 (5) (2008) 567–574.
- [6] M. Marquis, C. Beaubois, V.P. Lavallée, M. Abrahamowicz, C. Danielli, S. Lemieux, I. Ahmad, A. Wei, S.B. Ting, S. Fleming, A. Schwarzer, D. Grimwade, W. Grey, R.K. Hills, P. Vyas, N. Russell, G. Sauvageau, J. Hébert, High expression of HMGA2 independently predicts poor clinical outcomes in acute myeloid leukemia, *Blood Cancer J.* 8 (8) (2018) 68.
- [7] M.J. Wang, H. Zhang, J. Li, H.D. Zhao, microRNA-98 inhibits the proliferation, invasion, migration and promotes apoptosis of breast cancer cells by binding to HMGA2, *Biosci. Rep.* 38 (5) (2018) (pii: BSR20180571).
- [8] Y. Tian, N. Zhang, S. Chen, Y. Ma, Y. Liu, The long non-coding RNA LSINCT5 promotes malignancy in non-small cell lung cancer by stabilizing HMGA2, *Cell Cycle* 5 (2018) 1–11.
- [9] X.L. Gao, M.G. Cao, G.G. Ai, Y.B. Hu, Mir-98 reduces the expression of HMGA2 and promotes osteogenic differentiation of mesenchymal stem cells, *Eur. Rev. Med. Pharmacol. Sci.* 22 (11) (2018) 3311–3317.
- [10] M. Fedele, M. Fedele, V. Fidanza, S. Battista, F. Pentimalli, A.J. Klein-Szanto, R. Visone, I. De Martino, A. Curcio, C. Morisco, L. Del Vecchio, G. Baldassarre, C. Arra, G. Viglietto, C. Indolfi, C.M. Croce, A. Fusco, Haploinsufficiency of the Hmga1 gene causes cardiac hypertrophy and myelo-lymphoproliferative disorders in mice, *Cancer Res.* 66 (5) (2006) 2536–2543.
- [11] Q.Q. Wu, M. Xu, Y. Yuan, F.F. Li, Z. Yang, Y. Liu, M.Q. Zhou, Z.Y. Bian, W. Deng, L. Gao, H. Li, Q.Z. Tang, Cathepsin B deficiency attenuates cardiac remodeling in response to pressure overload via TNF-α/ASK1/JNK pathway, *Am. J. Physiol. Heart Circ. Physiol.* 308 (9) (2015) H1143–H1154.
- [12] Q.Q. Wu, et al., OX40 regulates pressure overload-induced cardiac hypertrophy and remodelling via CD4+ T-cells, *Clin. Sci. (Lond)* 130 (22) (2016) 2061–2071.
- [13] Q.Q. Wu, et al., Cathepsin B deficiency attenuates cardiac remodeling in response to pressure overload via TNF-α/ASK1/JNK pathway, *Am. J. Physiol. Heart Circ. Physiol.* 308 (9) (2015) H1143–H1154.
- [14] Y. Liu, Z. Hu, H.H. Liao, W. Liu, J. Liu, Z.G. Ma, Q.Q. Wu, M. Xu, N. Zhang, Y. Zhang, Z.Y. Bian, Q.Z. Tang, Toll-like receptor 5 deficiency attenuates interstitial cardiac fibrosis and dysfunction induced by pressure overload by inhibiting inflammation and the endothelial-mesenchymal transition, *Biochim. Biophys. Acta* 1182 (11) (2015) 2456–2466.
- [15] Y. Xi, W. Shen, L. Ma, M. Zhao, J. Zheng, S. Bu, S. Hino, M. Nakao, HMGA2 promotes adipogenesis by activating C/EBPβ-mediated expression of PPARγ, *Biochem. Biophys. Res. Commun.* 472 (4) (2016) 617–623.
- [16] L. Tao, et al., Exercise for the heart: signaling pathways, *Oncotarget* 6 (25) (2015) 20773–20784.
- [17] M. Kvandová, M. Majzúnová, I. Dvořáková, The role of PPARγ in cardiovascular diseases, *Physiol Res* 65 (3) (2016) S343–S363.
- [18] S. Polvani, M. Tarocchi, A. Galli, PPARγ and oxidative stress: con(β) catenating NRF2 and FOXO, *PPAR Res.* 2012 (2012) 641087.
- [19] S.Z. Duan, M.G. Usher, R.M. Mortensen, PPARs: the vasculature, inflammation and hypertension, *Curr. Opin. Nephrol. Hypertens.* 18 (2) (2009) 128–133.
- [20] A. Oyekun, PPARs and their effects on the cardiovascular system, *Clin. Exp. Hypertens.* 33 (5) (2011) 287–293.
- [21] J.E. Montanez, J.M. Peters, J.B. Correll, F.J. Gonzalez, A.D. Patterson, Metabolomics: an essential tool to understand the function of peroxisome proliferator-activated receptor alpha, *Toxicol. Pathol.* 41 (2) (2013) 410–418.
- [22] N.H. Son, et al., Cardiomyocyte expression of PPARγ leads to cardiac dysfunction in mice, *J. Clin. Invest.* 117 (10) (2007) 2791–2801.
- [23] S.Z. Duan, et al., Cardiomyocyte-specific knockout and agonist of peroxisome proliferator-activated receptor-gamma both induce cardiac hypertrophy in mice, *Circ. Res.* 97 (4) (2005) 372–379.
- [24] M. Asakawa, et al., Peroxisome proliferator-activated receptor gamma plays a critical role in inhibition of cardiac hypertrophy in vitro and in vivo, *Circulation* 105 (10) (2002) 1240–1246.
- [25] N.H. Son, S. Yu, J. Tuinei, K. Arai, H. Hamai, S. Homma, G.I. Shulman, E.D. Abel, L.J. Goldberg, PPARγ-induced cardiotoxicity in mice is ameliorated by PPARα deficiency despite increases in fatty acid oxidation, *J. Clin. Invest.* 120 (10) (2010) 3443–3454.
- [26] T. Tuomainen, P. Tavi, The role of cardiac energy metabolism in cardiac hypertrophy and failure, *Exp. Cell Res.* 360 (1) (2017) 12–18.
- [27] H.H. Liao, et al., The role of PPARs in pathological cardiac hypertrophy and heart failure, *Curr. Pharm. Des.* 23 (11) (2017) 1677–1686.
- [28] T. Nguyen, P. Nioi, C.B. Pickett, The Nrf2-antioxidant response element signaling pathway and its activation by oxidative stress, *J. Biol. Chem.* 284 (20) (2009) 13291–13295.
- [29] W. Hur, N.S. Gray, Small molecule modulators of antioxidant response pathway, *Curr. Opin. Chem. Biol.* 15 (1) (2011) 162–173.
- [30] Robert E. Smith, Kevin Tran, Cynthia C. Smith, Miranda McDonald, Pushkar Shejwalkar, Kenji Hara, The role of the Nrf2/ARE antioxidant system in preventing cardiovascular diseases, *Diseases* 4 (4) (2016) E34.
- [31] Q. Zhang, M.K. Ramlee, R. Brunmeir, C.J. Villanueva, D. Halperin, F. Xu, Dynamic and distinct histone modifications modulate the expression of key adipogenesis regulatory genes, *Cell Cycle* 11 (23) (2012) 4310–4322.
- [32] P. Boström, N. Mann, J. Wu, P.A. Quintero, E.R. Plovie, D. Panáková, R.K. Gupta, C. Xiao, MacRae CA, A. Rosenzweig, B.M. Spiegelman, C/EBPβ controls exercise-induced cardiac growth and protects against pathological cardiac remodeling, *Cell* 143 (7) (2010) 1072–1083.